Chem Soc Rev

ROYAL SOCIETY OF CHEMISTRY

REVIEW ARTICLE

View Article Online
View Journal | View Issue

Cite this: *Chem. Soc. Rev.*, 2021, **50**, 11032

Review and comparison of layer transfer methods for two-dimensional materials for emerging applications

Thomas F. Schranghamer,[a] Madan Sharma,[b] Rajendra Singh[b] and Saptarshi Das *[acd]

Two-dimensional (2D) materials offer immense potential for scientific breakthroughs and technological innovations. While early demonstrations of 2D material-based electronics, optoelectronics, flextronics, straintronics, twistronics, and biomimetic devices exploited micromechanically-exfoliated single crystal flakes, recent years have witnessed steady progress in large-area growth techniques such as physical vapor deposition (PVD), chemical vapor deposition (CVD), and metal–organic CVD (MOCVD). However, use of high growth temperatures, chemically-active growth precursors and promoters, and the need for epitaxy often limit direct growth of 2D materials on the substrates of interest for commercial applications. This has led to the development of a large number of methods for the layer transfer of 2D materials from the growth substrate to the target application substrate with varying degrees of cleanliness, uniformity, and transfer-related damage. This review aims to catalog and discuss these layer transfer methods. In particular, the processes, advantages, and drawbacks of various transfer methods are discussed, as is their applicability to different technological platforms of interest for 2D material implementation.

Received 24th July 2021

DOI: 10.1039/d1cs00706h

rsc.li/chem-soc-rev

Introduction

The discovery of graphene revolutionized research on two-dimensional (2D) layered materials,[1] prompting extensive study into electronic devices including transistors, photodetectors, sensors, *etc.*[2–9] Beyond graphene, semiconducting transition metal dichalcogenides (TMDCs),[10–13] and insulating hexagonal boron nitride (h-BN)[14,15] have also received significant attention from the electronic community. While early researchers believed that 2D materials could serve as a potential replacement for

[a] *Department of Engineering Science and Mechanics, Penn State University, University Park, PA 16802, USA. E-mail: sud70@psu.edu, das.sapt@gmail.com*
[b] *Department of Physics, Indian Institute of Technology Delhi, Hauz Khas, New Delhi 110016, India*
[c] *Department of Materials Science and Engineering, Penn State University, University Park, PA 16802, USA*
[d] *Materials Research Institute, Penn State University, University Park, PA 16802, USA*

Thomas F. Schranghamer

Mr. Thomas Schranghamer received his BS and MS degrees in Engineering Science and Mechanics from the Pennsylvania State University, USA, where he is currently a PhD candidate. His research interests lie in the development of novel device technologies utilizing low-dimensional materials such as 2D materials, particularly non-volatile memory devices for neuromorphic computing applications.

Madan Sharma

Mr. Madan Sharma is a research scholar at the Indian Institute of Technology Delhi. His research area is experimental condensed matter physics, with an emphasis on layer transfer of 2D materials for the fabrication of heterostructures and nanodevices. He received his MSc degree in Physics from Kurukshetra University. In 2018, he was awarded Inspire Fellowship to carry out his PhD studies.

traditional silicon (Si) in front-end-of-line (FEOL) technologies,[16] these hopes have been largely stymied by the growth requirements of high-quality, large-area 2D materials. For example, high temperatures in excess of 700 °C[17–20] are required to grow 2D semiconductors with reasonable carrier mobility (>50 cm^2 V^{-1} s^{-1}) *via* chemical vapor deposition (CVD) and metal–organic CVD (MOCVD) techniques. At such temperatures the growth process can have negative effects on the underlying substrate, hampering the reliability and performance of fabricated devices.[21–24] While the use of precursors such as salt can reduce growth temperature and improve growth quality, these precursors can themselves have unwanted effects (doping, contamination, *etc.*) on the substrate.[20,23,25] As a result, the fabrication of high-quality FEOL technologies based on 2D materials is currently dependent on layer transfer: the ability for high-quality 2D materials to be grown on a (growth) substrate and cleanly transferred to another (target) substrate for device fabrication. While promising, most layer transfer processes are time consuming, technically challenging, and can cause film/substrate damage and introduce contaminants, prompting further research to prove their viability in enabling 2D material-based FEOL technologies.[26]

Instead of FEOL integration, an attractive alternative that may allow rapid industrial adoption of 2D materials is back-end-of-line (BEOL) integration as peripheral devices and sensors. While BEOL applications impose less stringent requirements on device performance, processing temperatures cannot exceed 400 °C, thus making layer transfer of 2D materials almost inevitable since monolithic growth of 2D materials at such low temperatures remains a fundamental challenge.[23,26–31]

Beyond Si replacement (FEOL) and augmentation (BEOL), 2D material-based devices can serve the growing need for low-cost, low-power, and high-volume edge devices for the Internet of Things (IoT), a worldwide, interconnected network of everyday objects with embedded sensors.[23,32] However, IoT devices use a wide variety of low thermal budget substrates such as flexible polymers and glass with different compositions,[23,33–39] making direct growth of high-quality 2D materials for these applications difficult and thereby necessitating layer transfer from dedicated growth substrates.[19,40,41]

More recently, "van der Waals (vdW) heterostructures," *i.e.*, structures comprised of different 2D materials stacked upon one another and bonded solely through vdW forces, have drawn significant attention. While past efforts utilizing molecular beam epitaxy (MBE) to grow similar heterostructures with III–V and II–VI semiconductors have seen success,[42–45] the emergent properties of stacked 2D materials have renewed widespread interest in the field. Notably, this new generation of vdW heterostructures takes advantage of the clean (*i.e.*, dangling bond free) and unreactive surfaces of 2D materials[46–48] to create pristine interfaces between the various constituent layers, thereby allowing for the creation of electronic devices with vastly improved performance and unique functionalities. The newly-minted field of "twistronics"[49–51] based on such vdW heterostructures has revealed unprecedented opportunities for scientific innovations. This progress has largely been enabled by the ability to transfer 2D materials between substrates, allowing for easy stacking and twisting of layers with mismatched lattices and negating the need for carefully optimized growth conditions.[48,52] However, for the properties of vdW heterostructures to be fully realized, contamination and damage-free transfer is imperative. Therefore, it is clear that development of such clean, damage-free, and scalable layer transfer methods will be critical not only for industrial and commercial implementation of 2D materials, but also for research of novel physical phenomena and development of as-yet unknown technologies.

Concerning the development of layer transfer, several notable papers reviewing transfer methods have already been published. However, of these papers, most have remained relatively narrow in scope, pertaining to only a single

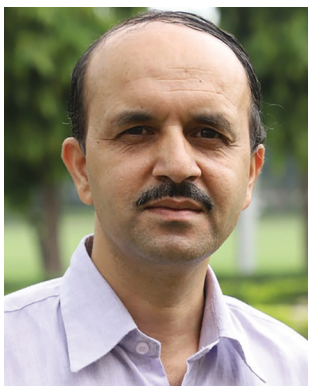

Rajendra Singh

Dr. Rajendra Singh is a Professor at the Department of Physics, IIT Delhi, New Delhi from 2006. He recieved PhD degree from the Inter-University Accelerator Centre (affiliated to J.N.U., New Delhi) in 2001. He worked as post-doctoral fellow first at the Walter Schottky Institute, Technical University of Munich, Germany and then at the Max Planck Institute of Microstructure Physics, Halle, Germany (2001–2006). His areas of interest are GaN-based materials and devices, wafer bonding, layer transfer of crystalline semiconductors and 2D materials, 2D materials and devices, 2D/3D heterojunctions. He has about 150 publications in International Journals and a similar number of publications in conference proceedings.

Saptarshi Das

Dr. Saptarshi Das is an Associate Professor in the Department of Engineering Science and Mechanics at Penn State University from 2016. He received PhD degree (2013) in Electrical and Computer Engineering from Purdue University. He was a Postdoctoral Research Scholar (2013–2015) and Assistant Research Scientist (2015–2016) at Argonne National Laboratory (ANL). Dr. Das was the recipient of Young Investigator Award from United States Air Force Office of Scientific Research in 2017 and National Science Foundation (NSF) CAREER award in 2021. His research interest includes 2D materials and devices for biomimetic sensing, neuromorphic computing, hardware security, flexible electronics, and straintronics.

material[53] or focusing on certain methods for specific tasks.[54,55] Therefore, there remains a critical need for a comprehensive discussion not only on the plethora of extant layer transfer methods but also their suitability across the various application platforms of interest for 2D materials, *i.e.*, FEOL and BEOL replacement/augmentation of Si-based technology, IoT edge devices/sensors, and vdW heterostructures. Thus, this review aims to provide a thorough overview of the various layer transfer methods for 2D materials and investigate their suitability for these applications. In particular, the impact of each method on the structural integrity and contamination of the transferred material is discussed, as are their scalability and any recent innovations, before analysing how they pertain to each application platform. We will also highlight the challenges still facing extant layer transfer methods and how they are being mitigated. Finally, we will conclude with a future perspective on the potential of layer transfer methods for the fabrication of 2D material-based novel electronic devices.

Assessment protocol for layer transfer methods for benchmarking

Fig. 1 highlights the importance of developing layer transfer methods to bridge the gap between high-quality growth of large-area (wafer-scale) 2D films and their eventual industrial adoption in various existing, emerging, and unforeseen technologies. At the same time, it is important to establish proper assessment techniques to rapidly and accurately characterize 2D materials before and after the transfer process to ensure quality control is retained. In addition to transfer speed and complexity, the post-transfer film cleanliness, defectivity, and uniformity, as well as the electronic and optoelectronic transport properties of nanoscale devices fabricated from the transferred films, can be used as benchmarking metrics to determine the strengths and weaknesses of different layer transfer methods. The purpose of this section is to simply establish the characterization techniques used to assess the quality of transferred films; a more thorough discussion of several characterization techniques and how they pertain to transferred films can be found in a recent review by Watson *et al.*[56]

For assessing the quality of both as-grown and transferred 2D materials, microscopy and spectroscopy characterization techniques are particularly preferred due to their non-contact and sub-micrometer spatial resolution. At the simplest level, optical microscopy typically offers a fast and easy way of estimating the coverage, cleanliness, uniformity, and thickness of transferred films (Fig. 2a). For situations where choice of substrate offers insufficient contrast for optical microscopy, ellipsometry may also be used to obtain similar information.[57] To ascertain information regarding the structural integrity and topography of transferred films, scanning electron microscope (SEM) (Fig. 2b) and transmission electron microscope (TEM) (Fig. 2c) imaging are high-resolution characterization options, capable of identifying the presence of nanometer-scale cracks, wrinkles, defects, and residues.[58–63] Atomic force microscopy (AFM) (Fig. 2d) is also often used to map pre- and post-transfer film morphologies, establishing the effects of transfer on film uniformity and cleanliness.[60,64,65] Most of these techniques are promising for non-destructive characterization of transferred 2D films, though techniques that utilize high-energy electron beams, such as high-resolution TEM, have been known to induce damage in 2D materials.[66–69]

Raman (Fig. 2e), photoluminescence (PL) (Fig. 2f), and X-ray photoelectron spectroscopy (XPS) (Fig. 2g) are all recognized as powerful optical characterization methods for identifying 2D

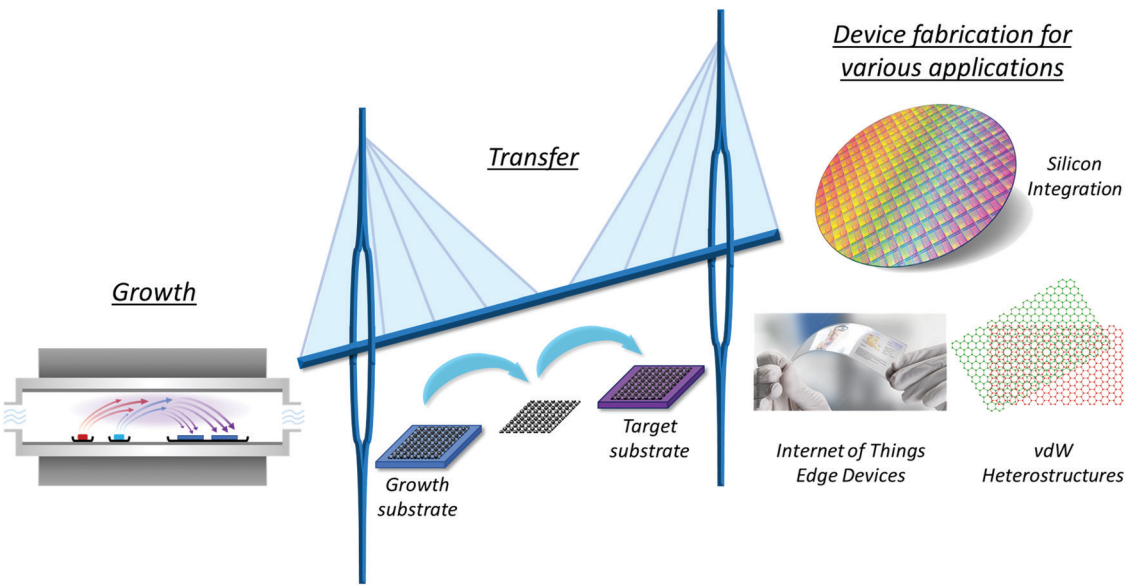

Fig. 1 Overview of the process flow necessary for implementation of 2D materials in commercial applications. In order to bridge the gap between the large area (wafer-scale) growth of 2D materials and fabrication of 2D devices for various potential applications, clean, uniform, and damage-free transfer of 2D materials from growth substrates to suitable target substrates must be developed.

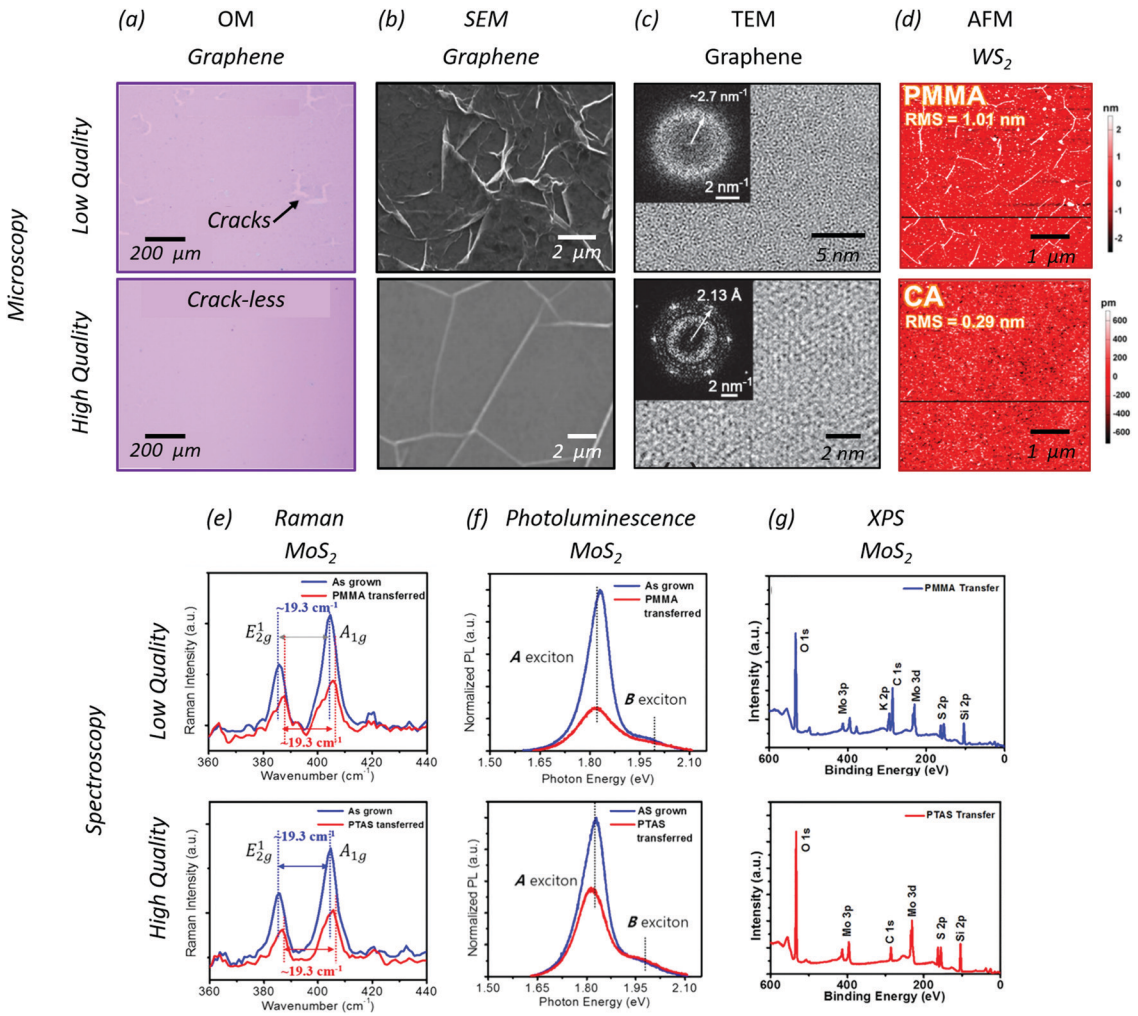

Fig. 2 Overview of microscopic and spectroscopic characterization methods to assess the pre/post-transfer quality of 2D materials. (a) Optical microscopy is used for quick and easy appraisal of film cleanliness and structural integrity. Cracks resulting from transfer can be seen in the top image. (b) Scanning electron microscopy (SEM) and (c) tunneling electron microscopy (TEM) are used to observe μm/nm-scale disorder indicative of damage/contamination. (d) Atomic force microscopy (AFM) is used to assess changes in step height indicative of cracks/wrinkles and/or contamination. The white lines seen in the top image are indicative of wrinkles in the transferred film. (e) Raman, (f) photoluminescence (PL), and (g) X-ray photoelectron spectroscopy (XPS) are used to assess the number of layers, presence of contamination, doping, and strain in 2D films. Steep, high magnitude peaks are indicative of high-quality and damage-free 2D material The full-width half maximum (FWHM) of spectra peaks corresponds directly to crystal quality. Large changes in FWHM before and after transfer, as seen in the top Raman and PL images, indicate degradation due to transfer. The peaks displayed in the XPS spectra denote the presence of different elements in the film; additional peaks following transfer thus demonstrate changes in chemical composition as a result of contamination. (a) adapted from ref. 82 with permission. © 2009 American Chemical Society. (b) adapted from ref. 60 with permission. © 2014 Elsevier Ltd. (c) adapted from ref. 59 with permission. © 2015 The Chemical Society of Japan. (d) adapted from ref. 61 with permission. © 2019 American Chemical Society. (e–g) adapted from ref. 67 with permission. © 2017 Elsevier B.V.

materials, and the number and uniformity of their constituent layers. The width and intensity of the characteristic peaks of these spectroscopy techniques are indicators of film quality, and can be correlated with disorder, contamination, doping, and strain induced by transfer.[28,41,59–61,64,70–72] Additionally, PL can provide a direct measurement of the layer-dependent bandgap for TMDCs.[28,73,74] More advanced characterization techniques, such as strain-induced second-harmonic generation[75] and terahertz time-domain spectroscopy,[76,77] are capable of mapping strain and electrical properties over large areas, respectively. While less common, contact angle measurements can also be used to indicate changes in surface chemistry following transfer; many 2D materials, such as MoS_2, are hydrophobic and naturally form high contact angles with water. Lower contact angles following transfer thus indicate increased hydrophilicity as a result of undesired chemical changes.[70]

Electrical characterization using fabricated devices is also used to assess transferred film quality to gauge the suitability of transfer methods for device fabrication. The key benchmarking parameters to use for assessment of 2D field effect transistor (FET) devices include field effect carrier mobility, current on–off ratio, threshold voltage, subthreshold slope, on-current, and, perhaps most importantly, hysteresis in the device characteristics measured both in air and under vacuum. Similarly, for photonic applications, parameters such as responsivity, detectivity, external quantum efficiency, and wavelength dependency

of optical response must be evaluated. While it is infeasible to assess all aspects of transferred films, the desired application platform must be kept in mind to determine which assessment techniques are best suited.

Nevertheless, using the above benchmarking metrics, we will next review several layer transfer methods including chemical-etchant assisted wet transfer,[78–80] etchant-free water-assisted transfer,[58,71,81] water-soluble layer-based transfer,[60,70,82] metal-assisted transfer,[65,83] and all-dry deterministic transfer.[48,52,72]

Layer transfer methods

Polymer-assisted transfer methods

Polymer-assisted transfer methods are summarized in Fig. 3. In these methods, the 2D film obtained on the growth substrate is coated with a polymer layer (Fig. 3a), most often a polymethyl methacrylate (PMMA) film, and delaminated from the substrate either using chemicals that etch the growth substrate (Fig. 3b) or by using capillary forces (Fig. 3c) or bubble formation (Fig. 3d), followed by fishing out the polymer/2D stack using the desired application substrate and removal of the polymer with chemical solvent treatment (Fig. 3e). The benefits and shortcomings of different polymer-assisted transfer methods are discussed below.

Chemical etchant-assisted wet transfer methods. Though its roots lie with the use of polymer supporting layers to transfer exfoliated graphene flakes between substrates,[84] the chemical-etchant assisted wet transfer method was first developed to transfer graphene grown *via* CVD on metal (Cu, Ni, *etc.*) foil as demonstrated by Reina *et al.*[79] in 2008. In this original transfer process, PMMA film is spun onto the surface of a graphene/Cu-foil stack to act as a mechanical supporting layer (Fig. 3a). Note that, while other polymers have also seen use in this capacity, PMMA remains commonly used due to its flexibility, high mechanical strength, water insolubility, stability against etchants, and easy removal in solvents.[53,79,80,85] The metal foil is then etched away by suspending the PMMA/graphene/metal stack on the surface of an etchant solution (Fig. 3a), such as iron(III) chloride ($FeCl_3$), hydrochloric acid (HCl), nitric acid (HNO_3), iron(III) nitrate ($Fe(NO_3)_3$, or copper chloride ($CuCl_2$).[86] Following this, the PMMA/graphene stack is cleaned using several de-ionized (DI) water baths and transferred onto the target substrate, with an acetone bath then being used to dissolve the PMMA support layer (Fig. 3e). As other 2D materials such as TMDCs grew in prominence, this transfer technique was quickly adopted for fabricating devices from large-area films grown using CVD.[87–93] This transfer method has proven to be both reliable and adaptable; in addition to transferring 2D films, transfer of pre-patterned nanostructures is also possible using this method, as demonstrated by Jiao *et al.*[78] and Lee *et al.*[94]

Instead of conventional etchants, strong bases like NaOH[95] and KOH[89] have also been used to delaminate TMDCs from growth substrates such as SiO_2 and are regarded as more attractive alternatives to highly hazardous and environmentally unfriendly HF, the use of which has been a major concern for the semiconductor industry since the early 1990s.[96] However, these chemical-assisted transfer methods can damage and dope the transferred film due to their corrosivity and chemical residues, respectively, leading to degradation in film quality and, ultimately, reduced device performance.[24,58,97–99] Additionally, etching of the growth substrate renders it unusable for subsequent growths, increasing the overall cost. As a result, reliance on this transfer method may limit industrial- and commercial-scale applications for 2D materials, necessitating the development of etchant-free layer transfer methods.

Etchant-free wet transfer methods. Several methods have been developed for etchant-free transfer of 2D materials. In particular, water-based methods that exploit capillary forces or interfacial bubble formation have seen particular interest.

The capillary force-driven methods operate off the penetration of water between hydrophobic 2D films and hydrophilic growth substrates, leaving the hydrophobic film attached to the polymer layer to float to the water surface (Fig. 3c). This method is simple and has seen significant interest due to near-total exclusion of damaging chemical treatments. The first such method was demonstrated by Schneider *et al.* in 2010.[100] This method, dubbed wedging transfer, allowed for delamination of 2D films/nanostructures, covered in a cellulose acetate supporting layer, from hydrophilic substrates immersed in a water bath at an angle of 30°.

The water was then pumped out, gradually lowering the sample onto a waiting target substrate. Once adhered, the supporting layer was removed using ethyl acetate. Despite its effectiveness, this particular method was noted to result in heavy crack/wrinkle formation due to trapping of water clusters/bubbles at the film/substrate interface unless the target is strongly hydrophobic.[101] Gurarslan *et al.*[71] later demonstrated another method in which a water droplet is placed onto a prepared polystyrene/2D/substrate stack, which is then manually cracked at the edges to promote water penetration. Delamination occurs, lifting the film to the surface of the droplet, which is then dried to permit a dry transfer of the film to a target substrate using tweezers. This method was successfully used to transfer MoS_2 and WS_2 off sapphire growth substrates onto SiO_2/Si for device fabrication with high structural integrity. Li *et al.*[102] demonstrated the use of a similar method to enable the transfer of various low-dimensional nanomaterials, such as nanoparticles, nanowires, and 2D films, as well as several kinds of nanostructures, including vdW heterostructures. However, later study indicated that high residual stress in the polymer supporting layer and the unconstrained capillary action seen in these methods could result in breakage of the support/film stack during delamination, indicating that a higher degree of control (precise delamination angles, gradual exposure to water, *etc.*) would be necessary for non-destructive transfer.[81]

In 2017, Zhang *et al.*[58] developed a more controlled capillary force-driven and etchant-free layer transfer method. In this method, PMMA is first spun onto a 2D-film/substrate stack

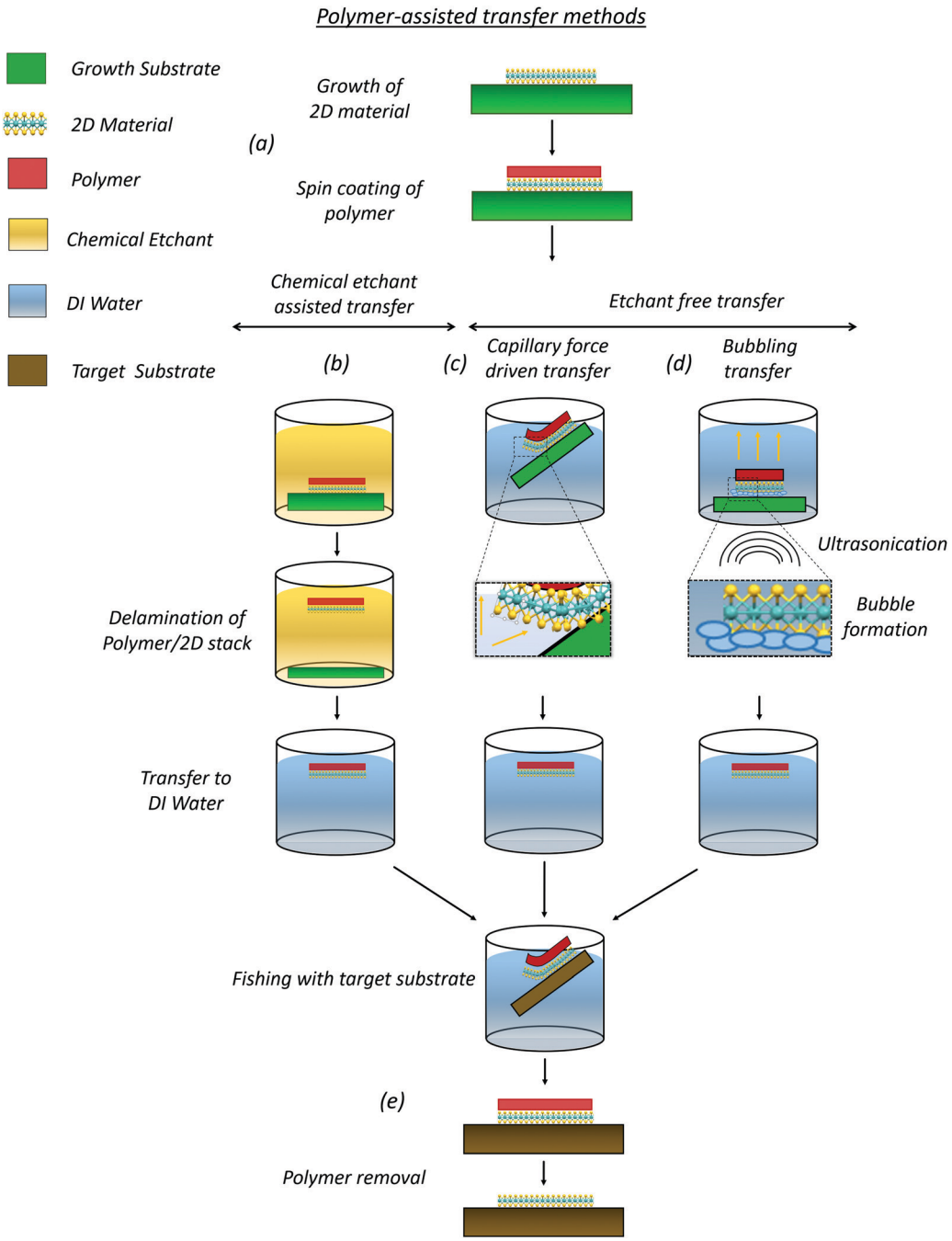

Fig. 3 Polymer-assisted wet transfer methods. (a) A polymer mechanical support layer is applied to the surface of an as-grown 2D film, typically *via* spin-coating. (b) Chemical etching transfer. The polymer/2D/substrate stack is immersed in an etchant solution. The material underlying the film is selectively etched, allowing for the film to delaminate and float to the surface of the solution. The film is then cleaned in deionized (DI) water and fished out using the target substrate. (c) Capillary-driven transfer. Differences in surface energy between the hydrophobic 2D film and hydrophilic growth substrate promote penetration of water at the interface between the two materials. The capillary force exerted by the penetrating water molecules pushes apart the film and substrate, causing the film to delaminate and float on the water surface. The film is then fished out using the target substrate. (d) Bubbling transfer. Hydrogen bubbles are generated at the film/substrate interface and subsequently collapse, providing sufficient energy to delaminate the film. After floating to the surface, the film is fished out using the target substrate. Note that while ultrasonic bubbling is shown here, electrochemical bubbling is also possible. (e) Following transfer to the target substrate, the polymer supporting layer is chemically removed using a solvent bath, leaving behind the transferred film.

and left overnight to ensure good adhesion between the PMMA and 2D film. Following this, the entire stack is immersed in hot DI water at an angle of $\sim 45^{\circ}$ with respect to the water surface. After a few seconds, the water begins to penetrate the film/substrate interface due to the capillary forces resulting in the delamination of the PMMA/2D-film from the substrate.

The delaminated film floats to the surface and is subsequently transferred onto another desired substrate. Finally, the PMMA layer is removed using acetone. This transfer method has been shown to work universally with several different TMDC/substrate combinations, including WSe_2 and MoS_2 grown on sapphire, TiN, and various glass substrates. This is notable as conventional etchants (*e.g.*, HF, NaOH, KOH) are not able to etch some common growth substrates (*e.g.*, TiN, sapphire) effectively, making it a challenging task to transfer 2D films from these substrates using the conventional chemical-etchant based methods. Another major benefit is that the substrate remains intact during this transfer process due to the absence of chemical agents, allowing it to be reused multiple times. Similar water-based transfer methods have been demonstrated for MoS_2 by Kim *et al.*[99] and Hong *et al.*[103] Notably, these methods eschew use of supporting layers, allowing for realization of extremely clean transferred films free of etchant-induced damage. However, analysis of the surface topography of these films displayed non-ideal protrusions and wrinkles, likely a result of a lack of mechanical support during pick-up using the target substrate. Trapped water clusters/adlayers were also noted, which can negatively affect fabricated device performance.[103]

Pre-treatment of the as-grown 2D film can also be used to ease delamination *via* capillary action. Wang *et al.*[104] demonstrated that transfer of WS_2 using a method similar to that developed by Gurarslan *et al.*[71] was significantly enhanced when binding between the CVD-grown monolayer and substrate (sapphire) was weakened using a two-step process. Temperature cycling using liquid nitrogen (N_2) served to weaken bonding due to differences in the thermal expansion coefficient between WS_2 (14.8×10^{-6} K^{-1}) and sapphire (4.5×10^{-6} K^{-1}), after which the sample was immersed in a Li ion solution to allow for Li ion intercalation between film and substrate, further weakening the TMDC–substrate interaction. Raman and PL mapping after each process noted a release in strain, which was taken to support the weakening of TMDC–substrate interactions, while post-transfer optical imaging indicated that this method resulted in improved transfer yield and reduced damage in the transferred film compared to untreated samples.

Etchant-free bubbling transfer methods, which utilize the formation of bubbles at the 2D/substrate interface as an external force promoting delamination, were originally developed to transfer graphene from metal foil. Hydrogen bubbles generated *via* water electrolysis were shown to delaminate graphene grown on Cu-foil in 2011.[105,106] The presence of a PMMA supporting layer was found to be vital for intact transfer using this method, as the shear forces produced during bubbling could easily shred the film without sufficient mechanical support. While nanoripples were identified in transferred films using this method, they were attributed to the surface topography of the Cu-foil growth substrate; as additional growth/transfer processes were performed, film quality improved due to gradual smoothening of the copper surface. The Cu-foil remained intact throughout several repeated transfer steps, establishing bubbling transfer as an environmentally-friendly and non-destructive alternative to chemical-etchant assisted wet transfers.[53] In addition to graphene on Cu-foil,[105] other studies have established the efficacy of this transfer method for other 2D material and substrate combinations, including graphene on Pt[105–107] and Ir-foil,[107] h-BN on Rh films,[108] and WS_2 and MoS_2/h-BN heterostructures on Au-foil.[109,110]

One recognized drawback of electrochemical bubbling is its reliance on a metal substrate, which functions as a cathode, to enable bubble formation at the substrate/2D interface.[55] Use of this method on other common growth substrates, typically insulators such as sapphire and SiO_2, is therefore infeasible. Thankfully, Ma *et al.*[59] has demonstrated a variant transfer method, referred to as ultrasonic bubbling transfer (Fig. 3d), for MoS_2 grown on a number of different substrates, including SiO_2, mica, sapphire, and strontium titanate (STO). In this transfer method, millions of micro-sized bubbles are generated by ultrasonication at the interface of the growth substrate and PMMA-coated MoS_2 inside a water bath. These bubbles collapse and produce sufficient force at the interface to delaminate the PMMA/MoS_2 stack from the underlying substrate. As previously discussed, the hydrophilic character of the growth substrates and the hydrophobic nature of PMMA and MoS_2 weakens the adhesion of MoS_2 to the growth substrate, making the separation of the PMMA/MoS_2 stack from growth substrate using this method easily possible. Characterization of the transferred films *via* optical and TEM imaging, as well as Raman and PL mapping, demonstrated that this method could be widely used to transfer MoS_2 and other TMDCs from various growth substrates without degradation of layer quality and morphology. Additionally, it was found that the delamination of MoS_2 films from the growth substrate takes less than one minute, establishing ultrasonic bubbling transfer method as a fast and efficient transfer process. Note that conventional wet transfer methods take more than 30 minutes for delamination of the PMMA/MoS_2 stack. Another significant advantage of this method is the recycling of the growth substrate due to a lack of chemical etching, allowing for the substrate to be reused in subsequent MoS_2 growth/transfer cycles.

Polymer-free transfer methods. While low-cost and straightforward, the transfer methods described above all rely on polymer (PMMA) adlayers to act as mechanical supports during transfer. Though these layers are removed using solvents at the end of the transfer process, significant amounts of polymer residue can still be found on transferred films. This residue, in turn, leads to non-ideal effects such as unintentional doping of the 2D film, severe hysteresis in the device characteristics, and reduced yield.[53,111] For example, PMMA residue has been shown to induce p-type doping in graphene and act as carrier scattering centers, thereby decreasing the carrier mobility of transferred graphene.[84,111,112] Various approaches have been implemented in attempts to mitigate this issue, such as through the addition of a second PMMA supporting layer[85,113] and by modification of the chemical structure of PMMA using UV radiation.[114,115] Post-transfer removal of residues has also been pursued through processes including annealing,[111,116,117] plasma treatment,[118] modified RCA cleaning[119] and mechanical

cleaning *via* conducting mode AFM.[120,121] A thorough discussion of the cleaning methods that have been applied to graphene, most of which have seen investigation for other 2D materials as well, can be found in a recent review by Zhuang *et al.*[122]

Alternatively, the tendency for residues to be left behind can be exploited to achieve desired electrical properties in transferred films. Lee *et al.*[123] demonstrated that fluoropolymers can serve as both a supporting layer and, once "removed" with a solvent, as a dopant; residue of the fluoropolymer CYTOP induced strong p-type doping in transferred graphene, reducing its sheet resistivity from its as-grown state. Similarly, it has been demonstrated that p-type doping of graphene by PMMA residue can be selectively controlled by changing the concentration of the PMMA solution.[112,113]

Recently, alternative supporting layer materials have been investigated such as cellulose acetate (CA),[64] paraffin,[124] rosin ($C_{19}H_{29}COOH$),[125] pentacene ($C_{22}H_{14}$),[126] polydimethylsiloxane (PDMS), and polystyrene (PS).[71,104,127–129] From a comparative study, it was found that CA films can be easily dissolved by acetone and leave considerably less residue when compared to PMMA. Moreover, TMDCs released from the substrate with a CA supporting layer were found to do so without bubble formation at the interface, which can be a major contributor to crack formation in transferred films. From post-transfer Raman, PL, and AFM measurements, it was found that the CA-transferred method preserved the quality of as-grown TMDCs better than PMMA-assisted layer transfer methods (Fig. 2d). However, as with conventional PMMA supporting layers, direct contact with the CA supporting layer was shown to induce physical damage such as cracks and holes in the transferred film. Thus, for damage-free and uniform transfer, such as that needed for industrial and commercial implementation of 2D materials, alternate transfer methods that either eschew the supporting layer entirely or offer greater mechanical support are of great interest.

Water-soluble layer transfer methods. First proposed by Cho *et al.*[70] for CVD-grown films, water-soluble layer transfer methods are etchant-free and support-layer-free transfer options (Fig. 4a) that have attracted interest in the 2D community for ultraclean transfer of 2D materials.[60,82,130,131] In this method, a water-soluble (sacrificial) layer is deposited on the growth substrate before the growth of a 2D film. Following growth, the complete film/soluble-layer/substrate stack is treated with DI water. The water-soluble layer dissolves,

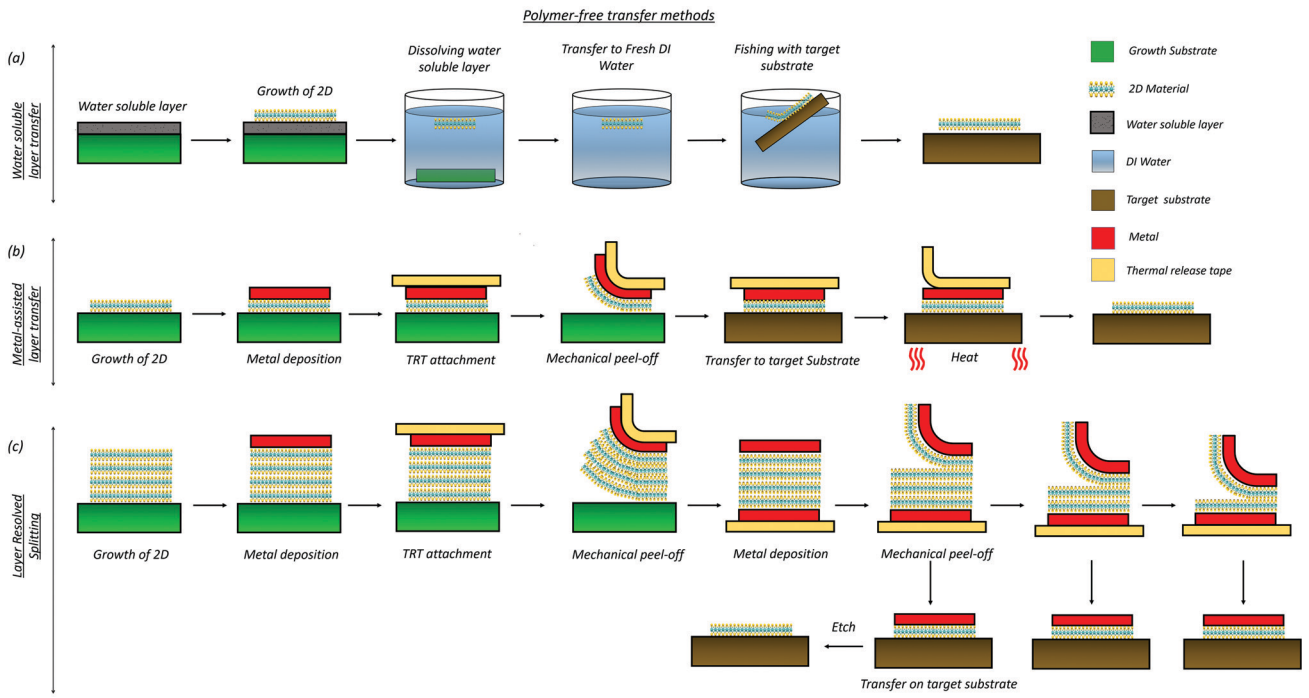

Fig. 4 Polymer-free transfer methods. (a) Water-soluble layer transfer. Prior to 2D film growth, a water-soluble layer (typically salt-based) is deposited on the growth substrate. The 2D material is then grown on the surface. The 2D/soluble-layer/substrate stack is then immersed in a water bath. The water-soluble layer dissolves, delaminating the film from the substrate and causing it to float to the liquid surface. The film is then transferred to a separate water bath to clean off residue from the soluble layer. The film is then fished out using the target substrate. (b) Metal-assisted transfer. A thin metal layer is deposited onto the as-grown 2D film. Thermal release tape (TRT) is applied to metal/2D/substrate stack and mechanically peeled, delaminating the TRT/metal/2D stack from the growth substrate. The stack is then pressed onto the target substrate. Heat is applied, allowing for easy removal of the TRT, and the metal layer is selectively etched, leaving behind the 2D film. (c) Layer-resolved splitting. A thin metal layer is deposited onto an as-grown multilayer 2D film. TRT is applied to metal/2D/substrate stack and mechanically peeled, delaminating the TRT/metal/2D stack from the growth substrate. The tape is then flipped, and another thin metal film is applied to the bottom 2D layer. This metal layer is then mechanically peeled, delaminating the bottom monolayer and allowing it to be pressed onto a target substrate. This process can be repeated *n*-times, where *n* is the number of layers in the original 2D film, in order to transfer the 2D material to *n* target substrates.

detaching the 2D film from the substrate. The floating film is then transferred onto the desired substrate in a similar manner to the wet transfers already discussed. Cho *et al.*[70] demonstrated this process using perylene-3,4,9,10-tetracarboxylic acid tetrapotassium salt (PTAS) as the sacrificial layer for growth/transfer of MoS_2. A comparative study of the PTAS-assisted transfer method with chemical wet-etching transfer (KOH) was conducted using Raman, PL, XPS, and contact angle measurements. In the XPS spectra (Fig. 2g), while all characteristics peaks of MoS_2 (Mo 3p, Mo 3d, and S 2p) were found to be similar for both transfer methods, an extra K 2p peak was noted for the etchant-assisted transfer method, which was attributed to change in the chemical composition of the MoS_2 film because of KOH etching. Additionally, careful examination of the O 1s peak revealed the presence of a metal oxide (M–O) bonding peak. This peak was believed to have occurred due to the etching of SiO_2 with KOH and cleaning of PMMA with acetone and was not found in the XPS spectra of the MoS_2 film that underwent PTAS-assisted transfer. XPS observations firmly indicate the superiority of PTAS-assisted transfer. These results were further supported by contact angle measurements. MoS_2 forms a high contact angle with water due to its hydrophobic nature. While a contact angle of $\sim 69.41^\circ$ was formed by the MoS_2 film transferred by the PTAS-assisted transfer method, the film transferred by the etchant-assisted method formed a contact angle of only $\sim 55.55^\circ$. The reduced contact angle is an indication of increased hydrophilicity of the MoS_2 film, likely due to M–O bonding on the film surface introduced by the etchant-assisted transfer method. In addition, excellent hydrogen evolution reaction (HER) performance was noted due to the damage, residue, and oxygen contamination-free PTAS-assisted transfer, indicating that this transfer method may be an attractive option for fabrication of TMDC-based energy harvesting devices such as hydrogen fuel cells.

Water-soluble layers like PTAS can also function as seed promoters and support the nucleation of large-area, continuous, and uniform 2D planar films on a variety of substrates.[130,132] In addition to PTAS, other salts have also been shown to be effective for enabling water-soluble transfer, either as the sacrificial layer[82,130] or as the primary growth substrate.[131] However, of these studies, several[82,130] were still forced to make use of PMMA supporting layers due to non-coalesced growth. Thus, while water-soluble transfer appears promising for future 2D development, it is apparent that greater progress is needed in ensuring large-area and conformal growth of materials is achievable with different sacrificial layers.

Metal-assisted transfer methods. Resist-free metal-assisted transfer methods have also been examined for clean transfer of 2D materials.[65,83,133–135] While similar techniques were previously utilized to isolate monolayer graphene from bulk graphite,[136] the intent for these novel transfer methods is to eliminate polymer contamination by utilizing metal thin films as supporting layers in place of PMMA or another polymer. Additionally, the greater adhesion between metals and TMDs, as well as the greater mechanical stiffness of metal films, allows for greater stability during transfer and thus greater structural integrity in transferred films. In 2015, Lin *et al.*[83] proposed a Cu-assisted transfer method by which a centimeter-scale MoS_2 thin film was transferred successfully (Fig. 4b). In this transfer process, a thin Cu film (thickness of ~ 60 nm) was deposited on as-grown MoS_2 by thermal evaporation. A piece of thermal release tape (TRT) was then gently pressed onto the Cu-coated substrate and peeled off, causing the MoS_2 film to delaminate from the underlying growth substrate (SiO_2). The TRT/Cu/MoS_2 stack was then pressed onto the target substrate, which was subsequently heated at 120 °C to allow the TRT to easily separate from the Cu film. The Cu film was then etched in a solution of ammonium persulphate ($(NH_4)_2S_2O_8$) and DI water and the MoS_2 film was subsequently cleaned using a modified RCA process.[119] Since the Young's modulus of Cu (~ 100 GPa) and MoS_2 (~ 270 GPa) are comparable, a Cu sacrificial layer, as opposed to conventional PMMA (Young's modulus of ~ 22 MPa), provides a more robust mechanical support to the MoS_2 film and reduces the generation of wrinkles and strain during the transfer process. In addition to Cu, gold (Au)[134] and nickel (Ni)[65,135] have also been used as robust mechanical support layers in metal-assisted transfer.

A variant metal-assisted transfer with similarities to the etchant-free wet transfer methods discussed previously was demonstrated by Lai *et al.*,[137] where intercalation of water *via* capillary action to delaminate a PDMS/PMMA/Cu/MoS_2 stack from the growth substrate was utilized. Compared to purely mechanical peeling, such as that utilized in TRT-based methods, this method demonstrated reduced crack and wrinkly formation as a result of mechanical support imparted by the buoyancy force of the water. The use of PDMS and PMMA supporting layers further protected the structural integrity of the films, with the Cu layer served as a barrier to polymer residue in addition to its already discussed benefits.

Metal-assisted transfer methods can also be used for the isolation of monolayers from multilayer films or removal of unwanted multi-layer islands from large-area monolayers as demonstrated by Shim *et al.*[65] Using a method known as layer-resolved splitting (LRS), originally developed for isolating graphene monolayers[133,135] and which utilizes differences in the interfacial toughness (Γ) of materials, it was possible to isolate and transfer wafer-scale (5 cm diameter) monolayers of 2D materials, including MoS_2, $MoSe_2$, WS_2, WSe_2, and h-BN (Fig. 4c). To split the layers apart, a 600 nm thick adhesive film of Ni was deposited on the as grown 2D material on sapphire substrate through vapor phase epitaxy. Ni was chosen due to the Γ between 2D materials and Ni ($\Gamma_{2D\text{-}Ni}$) being around ~ 1.4 J m^{-2}, higher than that between vdW layers of 2D materials ($\Gamma_{2D\text{-}2D} \sim 0.45$ J m^{-2}) and that between 2D materials and sapphire ($\Gamma_{2D\text{-}sapphire} \sim 0.26$ J m^{-2}).[138,139] As in other metal-assisted transfers, TRT was then applied to the top of the Ni film to act as a handler and the TRT/Ni/2D stack was mechanically peeled off the sapphire growth substrate. Next, another Ni layer was deposited on the bottom of the 2D film. A moment was then applied to the top Ni layer. Since $\Gamma_{2D\text{-}2D}$ is weaker than $\Gamma_{2D\text{-}Ni}$, the Ni/2D/Ni stack separated, leaving a monolayer of 2D material adhered to the bottom Ni film. This monolayer was then transferred onto a SiO_2/Si and the

Ni layer was etched away. This process can be repeated to separate as-grown multilayer 2D materials into their constituent monolayers, resulting in high yield.

The LRS method can also be used for the fabrication of wafer-scale heterostructures of 2D materials. In fact, h-BN/WS_2/h-BN and WS_2/h-BN heterostructures fabricated using the LRS method demonstrated 15-fold enhancement in PL intensity compared to conventional wet-etching transfer methods. Similarly, wafer-scale arrays of heterostructure devices consisting of MoS_2 and h-BN monolayers stacked using the LRS method on a SiO_2/Si wafer was able to demonstrate excellent device uniformity and low hysteresis.[65] These results indicate that the LRS method could represent an important step towards industrial-scale, high-throughput fabrication of monolayers and heterostructures of 2D materials.

While metal-assisted transfer methods have been shown to be effective for non-destructive and uniform transfer of 2D materials, they, like the polymer supported transfer methods described previously, remain limited by the need for chemical removal of the support layer. The harsh etchants used in this final step of the transfer process can damage or dope the transferred films, which can in turn affect device performance.[84,140] Imperfect etching/cleaning can also introduce metallic impurities in transferred films.[26,77] Additionally, the deposition methods used to form metal support layers need to be carefully considered; unprotected atomically-thin 2D materials can be easily damaged by energetic particles like free radicals seen in plasma-based deposition methods such as sputtering.[52,56,141–143] Factors such as deposition rate and energy need also be considered, as they directly affect the uniformity (microstructure) of the metal layer and its adhesion with the underlying 2D film.[144,145] Finally, metal support layers are etched away at the end of transfer and thus cannot be reused; this introduces additional expenses that would be detrimental for industrial-scale fabrication and is not environmentally friendly.

All-dry deterministic transfer methods. vdW heterostructures offer tremendous possibilities for studying intriguing science that can lead to the development of novel devices and unprecedented technologies. However, a key requirement for these discoveries is the need for atomically clean interfaces between the stacked layers. As a result, all-dry deterministic transfer has emerged as the premier transfer method for the fabrication of vdW heterostructures, based on the principles of viscoelastic stamping. In early iterations of this transfer method (Fig. 5a),[72] exfoliated flakes of desirable thicknesses were first identified both optically and through Raman spectroscopy. These flakes were then picked up using a viscoelastic stamp (PDMS) adhered to a glass slide mounted on a micromechanical stage with the stamp facing down. A microscope was used to optically align the desired flake with the target location, and the stage was lowered to press the stamp against the acceptor substrate, adhering the flake to it. The mechanical stage was then lifted very slowly to remove the stamp from the substrate. Due to the viscoelastic nature of the stamp, slow peeling allowed for the stamp to detach from the adhered flake, leaving it in the desired location. Deterministic transfer methods are capable of fabricating both vdW heterostructures by stacking flakes of different materials and freely suspended structures by placing flakes over micro-holes/divots. Yang *et al.*[116] demonstrated that this same technique could be successfully applied to transfer 2D flakes on pre-patterned source and drain electrodes, eliminating the need for any post-transfer lithography for device fabrication.

While the viscoelastic stamping technique introduced the concept of all-dry transfer methods, the utilization of PDMS stamps, while cleaner than sacrificial layers, was still found to result in trace adsorbates on the transferred 2D material layer. More recent investigations have led to the development of alternative (polymer-free) all-dry transfer methods, most notably the vdW pick-up transfer method introduced by Wang *et al.*[146] Using this method (Fig. 5b), exfoliated 2D flakes are transferred through their vdW interactions with other 2D materials such as h-BN. h-BN flake exfoliated onto a PDMS stamp act as a polymer-free adhesion site for the target 2D material. Optionally, a polypropylene carbonate (PPC) layer can be first applied to the PDMS stamp to act as a thermal release layer for the h-BN during later stages.[146,147] The stamp stack is then loaded onto the micromechanical stage and lowered until the h-BN contacts the flake targeted for transfer. Slowly raising the stage causes the flake to lift off from the substrate due to the adhesion force arising from the large contact area at the h-BN/2D interface. The h-BN/2D stack is then lowered onto the target substrate/location and released from the stamp. In the initial demonstration of this technique,[146] an h-BN/graphene/h-BN heterostructure device was fabricated that displayed room temperature mobility up to 140 000 $cm^2\ V^{-1}\ s^{-1}$, signifying the ability of this transfer method to fabricate extremely high-quality vdW heterostructure devices.

While the scale of vdW pick-up transfer is quite limited due to inherent limitations in flake size, Kang *et al.*[148] have demonstrated centimeter-scale transfer and assembly of TMDC heterostructures utilizing similar principles. A TRT/adhesive film is attached to an as-grown TMDC monolayer (L0) and peeled off, delaminating L0 from the growth substrate. The TRT/adhesive/L0 stack is then pressed onto the next TMDC layers of interest (L1, L2, *etc.*) and lifted off, each time peeling free the as-grown film due to the TMDC–TMDC vdW interaction being stronger than the TMDC–substrate interaction. Once the desired number of layers have been picked up, the stack is placed onto the target substrate and heated to release the TRT. The adhesive layer can then be chemically removed to reveal the assembled heterostructure. Note that while polymers (PMMA) are utilized as the adhesive layer in the report by Kang *et al.*, other conformal films including oxides (SiO_2, HfO_2) and metals (Au) can also be used in this capacity if avoidance of polymer residue is critical.[148]

Other variations of this transfer method have also been developed. The use of a relatively thick (>100 nm) h-BN flake allows for post-transfer isolation of the transferred 2D material layer *via* the lateral displacement of the h-BN flake upon application of sufficient tangential force.[149] Additionally, usage of a hemispherical PDMS stamp in-place of a flat stamp allows

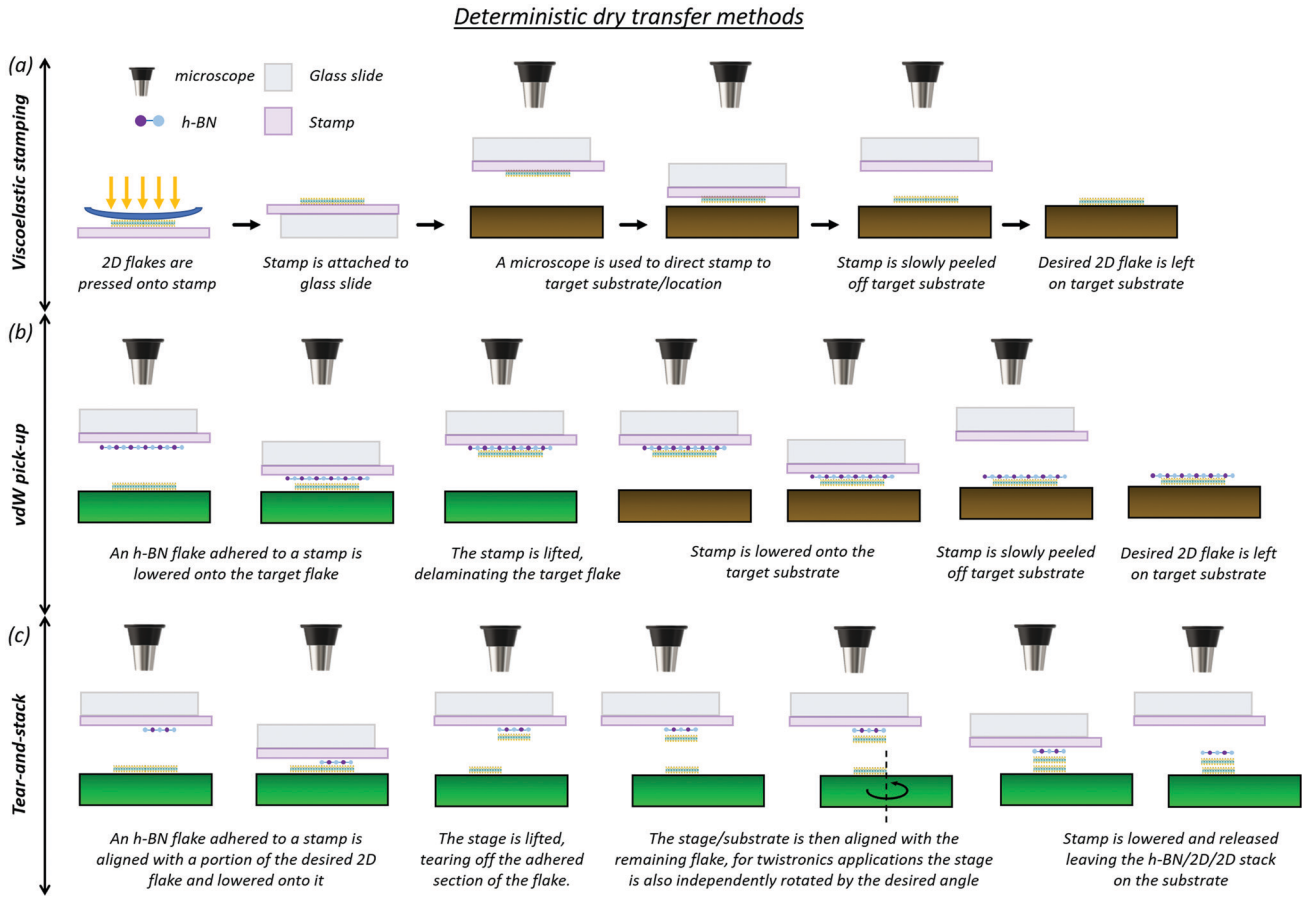

Fig. 5 Deterministic dry transfer methods. (a) Viscoelastic stamping transfer. The flake to be transferred is pressed/exfoliated onto a viscoelastic stamp (commonly PDMS). The stamp is then attached to a glass slide in a cantilever position. A micromechanical stage and optical microscope are used to align the flake with the target position and the stamp is lowered onto the target substrate, adhering the flake onto it. The stage is then slowly lifted, allowing the stamp to peel off the substrate without picking up the flake. (b) vdW pick-up transfer. A hexagonal boron nitride (h-BN) flake attached to a viscoelastic stamp is aligned with the desired 2D flake and lowered onto it. The stage is then slowly lifted; stronger vdW bonding between the flakes than between the flake and substrate ensures the desired flake remains attached. The h-BN/2D stack is then aligned with the target position and lowered onto the target substrate. The stage is then slowly lifted, releasing the flake stack. (c) Tear-and-stack transfer. A stamped h-BN flake is aligned with a portion of the desired 2D flake and lowered onto it. The stage is lifted, tearing off the adhered section of the flake. The stage/substrate is then independently aligned and/or rotated and the attached h-BN/2D stack is lowered onto the remaining as-grown portion. Finally, the stage is slowly lifted leaving the h-BN/2D/2D stack on the substrate.

for the introduction of a contact angle between the h-BN and target 2D material. This allows for better control of layer transfers (*i.e.*, h-BN onto graphene, the h-BN/graphene stack onto another material, *etc.*), preventing the formation of interfacial air/contaminant bubbles.[150] Several variations have also utilized alternative stamp materials, such as $ZnPS_3$ and $CrPS_4$, as a pick-up layer in-place of h-BN[151] and polycarbonate (PC)[152] and Elvacite[153] as stamp materials replacing PDMS. Stamp-less methods, such as the direct growth of h-BN on graphene and subsequent exfoliation to a target substrate,[154] have also been reported. Perhaps the most well-known and remarkable variant is the tear-and-stack method (Fig. 5c), most notable for its role in the recent development of the field of "twistronics". By initially picking up only half of a graphene flake, rotating it relative to the underlying substrate, and then placing it on the other half, the stacking angle can be altered arbitrarily and, at a specific "magic" angle ($\theta \approx 1.05^\circ$), superconductivity in bilayer graphene can be achieved.[49–51]

Despite their capabilities, the vdW pick-up transfer method and its derivatives possess a major drawback in the immense time investment required for the fabrication of each individual device, rendering wafer-scale arrays of vdW heterostructures a virtual impossibility for research settings. Automating the process is thus of immense interest for possible industrial-scale implementation. Current progress in this regard is discussed in more detail in *Layer transfer challenges and mitigations*.

Application specific requirements for transfer methods

The above discussion clearly highlights the benefits and shortcoming of various transfer methods. In this section we will assess the suitability of different transfer methods for specific technology platforms.

Replacement/augmentation of Si-based CMOS technology

As mentioned previously, layer transfer is currently regarded as integral for the realization of 2D material-based FEOL and BEOL applications. These applications range from replacement of Si as the primary channel material in complementary-metal-oxide-semiconductor (CMOS) technology (FEOL) to peripheral sensors, access transistors, and interconnect barriers (BEOL).[28,31] However, the drawbacks of layer transfer (time and material cost, technical complexity, potential contamination, damage to the film and target substrate *etc.*) have largely stymied industrial and commercial development of 2D materials for microelectronics. Thus, it is important to ascertain which transfer methods possess the greatest potential for high-performance device fabrication to facilitate future technological development. One of the key concerns of FEOL and BEOL integration is the introduction of contamination in the form of metal ions. Copper, gold, and silver ions are common contaminants that are highly mobile in SiO_2, forming deep trap states that can affect transistor performance in FEOL and lead to leakage/crosstalk between interconnects in BEOL.[26,155] The presence of these contaminants is a known issue with graphene grown on metal substrates, such as copper foil, but may also be extended to any 2D materials that interfaces with metals before completing transfer.[26,53,77,155–157] For this reason, it is unlikely that metal-assisted transfer is suitable for CMOS integration. Additionally, most forms of metal-assisted transfer are subtractive processes, requiring the use of metal etchants to remove the metal supporting layer following transfer to the target substrate. For various BEOL applications, this etch-step may severely impact the integrity of closely-packed metal interconnects. Other transfer methods that utilize etching are not exempt. Sodium (Na) contamination can be introduced due to the prevalence of NaOH as a chemical-etchant; like the metals previously mentioned, sodium contamination has historically been a source of mobile oxide charges in BEOL applications and a major cause of device performance loss.[158]

Etching-free transfer methods are thus more preferrable for large/industrial-scale transfer operations. In addition to eliminating the dangers of etchants and etchant residues to integrated circuit (IC) performance/reliability, removing the need for etch processes lowers fabrication costs by allowing for reuse of growth substrates and lowers waste production.[53,58] However, this can come at the cost of reduced structural integrity in transferred films because of reduced mechanical support, opening the way to mechanical failures that can negatively affect the device performance. Potential application of 2D materials as diffusion barrier layers for Cu interconnects may be disproportionately affected by crack, wrinkle, and defect formation in transferred films. These mechanical failures undermine the impermeable nature of 2D material barriers, allowing for enhanced diffusion and electromigration of interconnect metals, and vastly reducing IC reliability/lifetime.[28,53]

Deterministic transfer methods, while generally regarded as the cleanest, least damaging methods for transfer due to their conformal contacting, are severely restricted in regard to their maximum transferable area and long transfer time, making them ill-suited for wafer-scale fabrication.[26,146,159] Conversely, there have been several investigations into transfer methods compatible with roll-to-roll (R2R) processing for extremely large-scale fabrication of 2D material-based devices.[53,160–162] Further discussion regarding R2R transfer can be found in *Layer transfer challenges and mitigations*. Therefore, while several transfer methods show promise for damage- and contamination-free transfer of large-area uniform films, further improvement in their scalability is required to realize industrial-scale fabrication of 2D materials with Si.

2D material-based IoT devices

By 2025, the total number of devices incorporated within the IoT is expected to exceed 27 billion with a compound annual growth rate of 16% and a forecasted economic impact of 2–5 trillion dollars.[23] Ultra-thin 2D materials are well-poised to address several required areas of IoT hardware, especially flexible/wearable sensing and display electronics[163–168] and neuromorphic, biomimetic, and cryptographic edge devices.[41,169–180] However, a low thermal budget strongly prohibits the growth of most 2D materials on flexible and transparent substrates, including various glass and polymer substrates, necessitating the use of transfer methods for high-quality device fabrication. Depending on the substrate being utilized, different transfer methods may be more well suited than others. Organic polymers, such as poly(ethylene napthalate) (PEN), polyimide (PI), poly(ethylene terephthalate) (PET), polydimethylsiloxane (PDMS), *etc.*, inherently demonstrate high mechanical flexibility, stretchability, and durability; therefore these polymers are commonly used as substrates for flexible electronics.[181,182] However, most of these materials dissolve readily when exposed to acetone or other organic solvents, which are often used to dissolve the polymer supporting layer utilized in wet, water-soluble layer, and bubbling transfers.[53,60,79,80,85,181,182] Transfer methods that do not make use of polymer sacrificial layers, such as metal-assisted transfer and all-dry deterministic transfer, are thus promising for realizing non-destructive transfer to flexible substrates for IoT applications. Direct transfer from growth to application substrate (*i.e.*, transfer without any intermediate steps) is also promising for flexible electronic development. An etching-free wet transfer method similar to the wedging transfer pioneered by Gurarslan *et al.*[71] was used by Okogbue *et al.*[183] to directly transfer MoS_2 to a flexible application substrate. Pre-stretching of the target substrate allowed for controlled corrugation of a centimeter-scale transferred film, enhancing its mechanical flexibility/tunability. While similar 2D-to-3D nanostructures had been previously developed,[184] transfer to arbitrary substrates displayed significant crack/wrinkle formation, even with a metal mechanical support layer. Direct transfer to flexible substrates also shows promise for large-scale R2R processing, as will be discussed later. Despite the downsides of polymer supported transfers, variations may still be applicable for flexible electronic development. An *et al.*[185] developed a reverse transfer procedure based on chemical wet-etching, in which, after etching of the growth substrate and cleaning in DI water, the PMMA/graphene stack is flipped over and the PMMA layer is non-sacrificially adhered to the flexible target substrate. Consequently, no extra process is needed to dissolve the PMMA

layer, little contamination is introduced, and the presence of the PMMA interlayer serves to enhance adhesion of the film to the substrate.

Compared to polymer-based flexible-substrates, glass substrates are less prone to deterioration during solvent application, making a wider selection of transfer methods applicable. However, PMMA-less transfer methods remain preferable, owing to the significant effects of polymer contamination on chemical sensing (gas, biomolecule, *etc.*) and optoelectronic applications. For example, polymer residues can dope the 2D material, leading to inaccurate and unreliable sensor readout.[8,9,13,28,32,186] In optoelectronic devices, residues can lower quantum yield and device stability by significantly increasing surface roughness and reducing transparency, a phenomenon exacerbated in multilayer heterostructures like photovoltaic cells.[53,187] For other IoT sensing applications, such as touch sensors for display panels or strain sensors for micro-/nano-electromechanical systems, clean transfer is not as crucial, though device uniformity requirements still make damage-free transfer preferred.[188] Additionally, several etchants used in chemical-etching wet transfer, including HF[189] and HCl,[190] are known to have corrosive effects on glass. Etchant residue on transferred films may thus negatively affect substrate integrity/transparency, further reducing device performance. Concerning the viability of large-area transfer, IoT devices possess similar limitations to Si-based technologies; as transfer area scales up, there tends to be greater trade-off between cleanliness and post-transfer uniformity. An exception to this is that flexible substrates have greater compatibility with R2R processing than the rigid substrates used in traditional Si/CMOS-based technology.[160,162] Less stress is generated at the film/substrate interface during transfer, resulting in fewer structural defects forming and a more uniform post-transfer film. Of course, R2R transfer to more rigid glass substrates displays similar defect generation as to Si wafers, limiting the universal applicability of these transfer methods for IoT development.[53,161]

vdW heterostructures

The central criterion for unravelling the true potential of vdW heterostructures is the realization of pristine interfaces between the various constituent 2D layers. While past efforts utilizing molecular beam epitaxy (MBE) to grow similar structures with III–V and II–VI semiconductors have seen success,[42–45] layered 2D materials are currently thought to possess significant potential owing to their ability to be easily transferred between substrates. This allows for easy stacking of layers with mismatched lattices, negating the need for carefully optimized growth conditions. So far, successful vdW heterostructure based devices include transistors,[191,192] memory cells,[193] and photovoltaics.[194] While further development of novel vdW heterostructures is important for the commercial development of 2D materials and the observation of new physical phenomena,[47,54] most large-area transfer methods, such as conventional wet etching and water-soluble layer transfer, are not well-suited for the fabrication of vdW heterostructures. The use of sacrificial polymer support layers (*i.e.*, PMMA) often leads to the introduction of surface residues on the transferred 2D materials, sullying the otherwise pristine 2D/2D interfaces.[72] Similarly, metal support layers[65,83,134] can leave behind metallic particles, which can also degrade the interfaces and jeopardize the lifetime/reliability of devices *via* particle migration. Another issue is that the chemicals and capillary forces involved in the wet stage of these transfer methods can cause alterations in surface chemistry and/or the formation of cracks and wrinkles, worsening the quality of individual 2D layers.[81,84,97–99,105,140] As vdW heterostructures also require precise placement of each constituent layer, both with respect to the position of the underlying layers and to their lattice orientation,[195] the deterministic transfer methods discussed previously are believed to be the most promising for fabrication and development of vdW heterostructures at the industrial and commercial levels. However, the scalability of these transfer methods remains a major challenge. While the vdW pick-up method is often regarded as the cleanest deterministic transfer method, its reliance on hBN flakes imposes an intrinsic limit on the size of materials that can be transferred.[54] Additionally, locating and retrieving hBN flakes drastically increases the time needed to perform each transfer. Conversely, direct viscoelastic stamping using PDMS or another polymer allows for relatively rapid transfer of larger-area flakes, though overall cleanliness/uniformity decreases due to contact between the 2D material and polymer.[54] While dry transfer methods such as that developed by Jian *et al.*[148] appear extremely promising for clean, large-scale heterostructures, further improvements in transfer are needed for commercially-viable and industrial-scale development of high-performance vdW heterostructures.

Layer transfer challenges and mitigations

Across all transfer methods discussed, several universal challenges remain to be solved. Interfacial contaminants between the transferred material and substrate (or underlying 2D layer in the case of vdW heterostructures) are a major issue; small contaminant concentrations can drastically affect the surface roughness and electrical characteristics of adjacent 2D layers, making their elimination a top priority for high quality device fabrication.[48,52,53,196,197] Potential contaminants can stem from several sources, including water/oxygen molecules trapped during transfer,[53,103,148,198–201] adatoms introduced from the growth substrate and/or during etch processes,[155,202] hydrocarbons originating from air and/or imperfectly cleaned surfaces,[54,148,201,203,204] *etc.* In the case of vdW heterostructures, as a transferred layer adheres to the underlying layer, these trapped contaminants can spread out, with large pockets (μm-scale) separating into isolated bubbles (nm-scale). This process has been attributed to squeezing from the interlayer vdW forces.[54,204] Post-transfer thermal annealing (200 °C) has been shown to reverse this segregation in the case of graphene/h-BN heterostructures, with smaller contaminant

bubbles aggregating into larger, taller pockets. Higher temperature annealing (500 °C) led to greater aggregation of contaminants and, ultimately, rupture of the resulting pockets. In both cases, the generation of large, flat plains of graphene due to contaminant migration resulted in an improvement in electrical characteristics, namely an increase in mobility.[54,196] Performing deterministic transfers at slower speeds (<1 μm s^{-1}) and at higher temperatures (>70 °C) has been shown to reduce contamination trapping; the higher temperature increases the motility of contaminants while the slow adhesion process pushes the contamination out through vdW forces.[205] Introduction of a contact angle between the flake being transferred and the underling flake/substrate has also been shown to reduce interfacial bubble formation, as recently demonstrated by Iwasaki *et al.*[150] using a modified vdW pick-up process. A viscoelastic stamp with a hemispherical protrusion was utilized; by slowly picking up flakes near the edge of the protrusion, a controlled contact angle was able to be introduced between the transferred flakes and target substrates. Subsequently lowering the flakes in this manner served to aid in pushing out contamination using vdW forces, leaving the interfaces pristine with a >90% success rate. This was confirmed using optical microscopy, to identify structural changes from bubble formation, and quantum Hall effect measurements, to identify doping from contaminants. As air is a prominent source of interfacial contaminants (oxygen molecules, water vapor, airborne hydrocarbons, *etc.*), performing transfer under vacuum naturally aids in preventing the formation of contaminant bubbles. In the centimeter-scale heterostructure fabrication demonstrated by Kang *et al.*,[148] discussed previously, stacking of the constituent 2D layers in a vacuum chamber showed severely reduced bubble formation as opposed to stacking in an ambient environment. Post-transfer AFM imaging of vacuum-transferred MoS_2 showed a flat surface topology, while X-ray diffraction measurements indicated reduced interlayer spacing characteristic of pristine interfaces. Removal of interfacial contamination and voids through mechanical cleaning with contact-mode AFM has also seen attention. Rather than directly scraping off contaminants, as with AFM-based removal of PMMA residue,[120,121] the AFM tip is instead used as a "nano-squeegee," pressing on upper layers to squeeze out trapped contaminants and air bubbles, flattening the film's surface.[206,207] While this method has been shown to be effective in removing nanoscale interfacial bubbles, the AFM tip radius is too small to effectively treat micrometer-scale pockets such as those achieved *via* thermal annealing. This, combined with its overall low throughput (~ 6 μm^2 min^{-1} [207]), limits the applicability of this technique for industrial-scale fabrication efforts. For other large-area, non-heterostructure applications of 2D materials, surface treatment of the substrate prior to transfer stands to severely reduce or eliminate water adsorption at the interface. One example is the use of phenyl-terminated organosilane self-assembled monolayers on the underlying dielectric, which resulted in improved mobility and hysteresis of graphene FETs.[201,208]

Due to the numerous steps required for most layer transfer methods, the environmental conditions during transfer can be difficult to control. This is relevant not only for avoiding surface/interfacial contaminants,[48,52,53,196,197] but also for working with materials that rapidly degrade upon exposure to air and/or moisture. A large number of 2D materials, with some prominent examples being black phosphorus (BP),[209,210] molybdenum ditelluride ($MoTe_2$),[211,212] and niobium diselenide ($NiSe_2$),[54,210] have been shown to rapidly deteriorate under ambient conditions, largely limiting 2D material exploration to more chemically inert options such as graphene, h-BN, and certain TMDCs (MoS_2, $MoSe_2$, WS_2, *etc.*).[210,212,213] However, even these materials are believed to suffer from oxidation effects at extremely thin (monolayer/bilayer) thicknesses; as the materials are thinned, the effects of various adsorbed molecules on electrical characteristics become more pronounced.[54] MoS_2 has been shown to develop needle-like protrusions ranging 20–50 nm when exposed to water for times ≤ 1 h. XPS and atomic absorption spectroscopy (AAS) analysis of these formations have indicated them to likely be $MoO_3 \cdot H_2O$ crystals formed due to oxidation.[213,214] Regarding transfer, this indicates that deterioration from water-based oxidation may arise during cleaning processes, especially when handling extremely thin films. Use of dry transfer methods, such as the deterministic transfer methods discussed previously, would eliminate the danger of direct water exposure but would likely be insufficient for preventing deterioration from ambient moisture during the transfer process. In the development of their transfer process, Jiang *et al.*[148] noted that oxidized TMDC films produced significantly lower yield when etchant-free transfer methods (mechanical peeling and capillary-driven) were utilized. This was attributed to stronger binding between active sites in the film and the growth substrate, leading to tearing and separation of the film during delamination. As even cutting-edge glovebox chambers can only reach partial oxygen and water pressures of approximately 10^{-4} mbar,[54] damage from environmental conditions during transfer is likely to be a major limiting factor for future development regardless of transfer method.

For 2D materials to be implemented at an industrial scale for commercial applications, automated fabrication processes are needed. Given that the transfer methods are tedious and mechanically complex processes, automation remains a challenge. Recently, Han *et al.*[131] were able to demonstrate a semi-automated transfer process for the fabrication of vdW heterostructures using a home-made mechanical apparatus (Fig. 6a). However, as-of-yet, this approach lacks the high degree of control needed for fabricating vdW heterostructures such as those needed for implementing twistronics. Masubuchi *et al.*[153] have recently demonstrated an autonomous robotic system capable of performing vdW pick-up transfer (Fig. 6b). A high-speed optical microscope and motorized XY stage are used to scan an array of exfoliated substrates, optically identifying 2D flakes of a desired thickness through a computer vision algorithm. Flake parameters such as size, shape, and position are then recorded in a dedicated database. Using this information, computer-assisted design (CAD) schematics of device arrays and heterostructures based on the identified flakes can be prepared. These schematics are transferred to a robotic arm/stamping apparatus, which utilizes the same computer-vision algorithm to

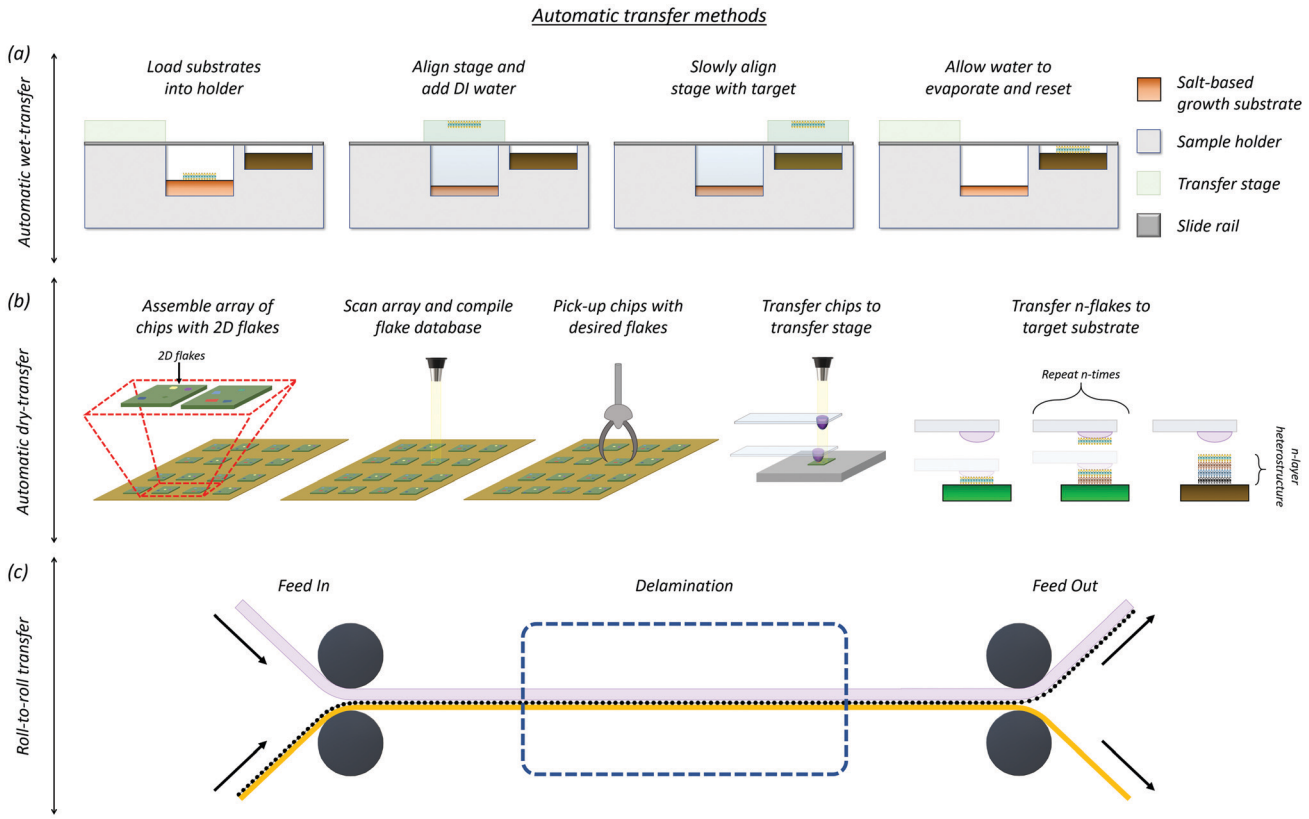

Fig. 6 Automated transfer methods. (a) Automated wet transfer. Growth and target substrates are loaded into the sample holder. The transfer stage is aligned with the growth substrate and deionized (DI) water is pumped in. The water-soluble growth substrate (salt-based) partially dissolves, delaminating the as-grown film and allowing it to float to liquid surface. The transfer stage is then slowly aligned with the target substrate, carrying along the floating film. The water is allowed to evaporate, gradually lowering the water level and depositing the film onto the target substrate. The transfer stage is reset, allowing the growth and target substrates to be retrieved. (b) Automated deterministic transfer for heterostructure fabrication. A chip tray is prepared with an array of substrates carrying isolated 2D flakes. The tray is autonomously scanned with an optical microscope system and a database of flakes meeting desired criteria (size, thickness, *etc.*) is compiled. Flakes are chosen from the database to fabricate desired van der Waals (vdW) heterostructures using a computer-assisted design (CAD) system/software. Based on which flakes are chosen, a robotic arm retrieves the necessary substrates and moves them to a designated transfer stage. The optical microscope system is again used to align an automatic stamping apparatus, which then retrieves the desired flakes and assembles the desired heterostructure on the target substrate. (c) Automated roll-to-roll transfer for flexible substrates. Target flexible substrate and metal foil growth substrate, shown here as copper carrying graphene, are fed into the system using rollers. The target and growth substrates are pressed together, adhering the 2D film to both. Delamination is induced between the film and growth substrate using methods such as chemical etching and electrochemical bubbling, leaving the film preferentially adhered to the target substrate. The substrates are fed out of the system, with the film now adhered to the target substrate.

retrieve specific substrates, locate desired flakes, and individually transfer flakes to create vdW stacks suitable for device fabrication. This system can autonomously identify $\geq$400 monolayer graphene flakes per hour at an error rate of $\leq$7% and has been used to prepare heterostructures containing up to 29 layers of 2D materials, indicating potential for industrial scale heterostructure fabrication. Additionally, the entire system is containable in a single glovebox, lowering the dangers of environmental degradation for various 2D materials as discussed previously. However, improvements still need to be made regarding alignment accuracy ($\pm1^\circ$ and ±1 μm, with human intervention) and interfacial contamination, as well as automation of the exfoliation and substrate preparation processes, for this technology to be widely implemented.

For large-area, non-heterostructure applications, implementation of roll-to-roll (R2R) processing has been achieved for transferring graphene (Fig. 6c), taking advantage of its ability to be grown on flexible metal foil. TRT was used by Bae *et al.*[160] to achieve the first R2R processing of graphene in 2010, transferring 30 inch monolayer films onto a flexible PET substrate. However, this process sports several significant disadvantages, including prominent damage generation when transferring to rigid substrates due to high interfacial stresses, contamination in the form of tape (polymer) residue, and high cost due to an inability to reuse tape.[53] To address these issues, PDMS supporting layers have also been used to realize continuous R2R transferring in a manner similar to the use of PDMS stamps in deterministic transfers. Advantages of this method include greater conformality during transfer, leading to less damage in transferred films, and low cost. As with PDMS stamping, a high degree of control is need for efficient implementation of this process; transfer yield is strongly

dependent on PDMS peeling rate and slip can easily occur due to the relatively weak adhesion between PDMS and graphene.[53] To reduce cost, eliminate contamination, and simplify the process even further, R2R transfer of graphene directly between the growth substrate and a target flexible substrate has also been investigated. While the high sheet resistance (2 kΩ sq^{-1}) of the first demonstration by Han *et al.*[162] indicated significant structural damage in the transferred film, more recent efforts have made use of adhesion/wetting enhancing interfacial layers on the target substrate.[215,216] Etching-free variants that utilize other transfer mechanisms, such as direct transfer *via* electrochemical bubbling[188,217] or capillary action,[218] have also been developed in pursuit of contamination-free and reusable R2R processing. Oxidation of the metal growth substrate has also been shown to be effective at enabling easy delamination of as-grown films; in the case of copper foils, intercalation of water at the interface leads to accelerated oxidation/corrosion of the copper surface, allowing for clean, non-destructive peeling *via* polymer support layers.[219–221] The simplicity and scalability of this method indicates high potential for industrial-scale fabrication, while the ability to freely reuse substrates indicates high commercial potential. For applicability to rigid substrates like SiO_2/Si, Shivayogimath *et al.*[222] have demonstrated a two-step R2R process using this method in which large-area graphene can be transferred from the growth substrate (Cu-foil) to a mechanically stable polymer support layer (PVA/paper stack). This stack can then be freely transported to the target substrate and applied without fear of damage from interfacial stresses. Remaining issues for implementation of R2R transfer on an industrial scale include insufficient study of the effects of underlying adhesive layers and poor scalability to multilayer heterostructures.[53] Additionally, all of the research discussed is oriented towards CVD-grown graphene only; large-area R2R transfer of other CVD-grown 2D materials, such as TMDCs, has yet to be investigated at a comparable scale. While there have been several demonstrations of centimeter-scale production of MoS_2,[223] WS_2,[109] and h-BN,[217,222] R2R production of non-graphene 2D materials remains largely limited to exfoliated sheets of nanoflakes, such as those demonstrated for MoS_2 by Oakes *et al.*[224] and Wells *et al.*,[225] or those grown *via* non-CVD methods on metal foil, such as thermal decomposition.[226]

Conclusion and future perspective

The last decade has seen significant progress in the development of transfer methods for 2D materials. The structural integrity of transferred films has greatly improved through thorough analysis of damage origins and mechanisms, which have facilitated the implementation of novel, damag-free transfer methods. Innovations in supporting layer materials have been developed to promote clean transfers, while polymer-free and all-dry transfer methods show great potential for eliminating the surface residue and interfacial contamination that have long plagued 2D material applications. Concurrently, progress has been made to achieve scalable and automated realization of transfer for industrial-scale fabrication efforts. However, certain challenges remain to be solved for potential 2D material applications to meet or exceed the standards set by conventional technologies. Part of this lies with improving growth processes; intrinsic defects, impurities, and grain boundaries often act as centres of structural damage and contamination during transfer of 2D films. Therefore, growth of uniform, clean, and monocrystalline films remains a prerequisite for eventual realization of high-quality, damage- and contamination-free transfer over large areas. Regarding the transfer methods discussed, structural damage continues to inhibit transfer of large-area films, particularly in the cases of transfer methods that aim to reduce contamination by eliminating sacrificial support layers. Going forward, easing the delamination process will be a key step in ensuring damage-free transfer and will be particularly attractive for mechanically-intense methods such as R2R transfer of films to-or-from rigid substrates. In turn, this could allow for more effective R2R transfer of 2D materials other than graphene, including TMDs, with higher post-transfer quality and yield. Potential approaches in this respect include pre-treatment of the growth substrate and modification of the growth process to weaken the 2D/substrate interactions. Extant water-soluble layer transfer methods already demonstrate the validity of these approaches. Conformal contacting of 2D films with the target substrate is also critical for eliminating post-transfer damage. Cracks and wrinkles often form where interfacial contamination or insufficiently robust supporting layers prevent films from adhering directly to the substrate. As discussed, pre-treatment of the target substrate, precise control over the transfer process (speed, angle of approach, environmental conditions, *etc.*), and investigation of novel supporting materials all show great promise for remedying this issue. Of course, it becomes much more difficult to tackle these challenges as the area of the transferred film is scaled up, often making it necessary to compromise between having clean films and having uniform, damage-free films. Due to the mechanical limitations of retrieving and placing extremely large-area films, investigation and development of novel supporting layers capable of enabling both clean and uniform transfer is likely needed to realize wafer-scale fabrication compatible with modern processing lines. A simplistic process similar to the traditional wet-etching and water-soluble layer transfer methods is preferred for ensuring reliable, uniform, and reproducible transfer across the entire area, while also making the process implementable at an industrial-scale with minimum human oversight and few mechanically complex steps. Such a process also lends itself easily to the technological platforms of interest for 2D materials; BEOL, IoT, and vdW heterostructure applications would all benefit immensely from clean and uniform transfer of large-area films.

Author contributions

All authors contributed to the preparation of the manuscript.

Conflicts of interest

The authors declare no competing financial interest.

Acknowledgements

Authors would like to thank Mr. Abu Musa Abdullah for his help with the preparation of the figures. Mr. Thomas F. Schranghamer and Dr. Saptarshi Das would like to thank the Army Research Office (ARO) for funding support through Contract Number W911NF1920338 and the National Science Foundation (NSF) through the CAREER Award under Grant Number ECCS-2042154. Mr. Madan Sharma would like to express his gratitude to the Department of Science & Technology (DST) for the award of the Senior Research Fellowship (SRF). Dr. Rajendra Singh is thankful to the Ministry of Human Research Development (MHRD) and IIT Delhi for partial funding support from the Grand Challenge Project "MBE Growth of 2D Materials" under Grant Number MI01800G.

References

1 K. S. Novoselov, *et al.*, Electric field effect in atomically thin carbon films, *Science*, 2004, **306**(5696), 666–669.
2 S. K. Banerjee, L. F. Register, E. Tutuc, D. Reddy and A. H. MacDonald, Bilayer pseudospin field-effect transistor (BiSFET): A proposed new logic device, *IEEE Electron Device Lett.*, 2008, **30**(2), 158–160.
3 S. Kim, *et al.*, Realization of a high mobility dual-gated graphene field-effect transistor with Al_2O_3 dielectric, *Appl. Phys. Lett.*, 2009, **94**(6), 062107.
4 M. C. Lemme, *et al.*, Mobility in graphene double gate field effect transistors, *Solid-State Electron.*, 2008, **52**(4), 514–518.
5 K. L. Wong, *et al.*, Carrier transport of rough-edged doped GNRFETs with metal contacts at various channel widths, *Superlattices Microstruct.*, 2020, **143**, 106548.
6 S. Basu, M. C. Lee and Y.-H. Wang, Graphene-based electrodes for enhanced organic thin film transistors based on pentacene, *Phys. Chem. Chem. Phys.*, 2014, **16**(31), 16701–16710.
7 Z. Zhu, I. Murtaza, H. Meng and W. Huang, Thin film transistors based on two dimensional graphene and graphene/semiconductor heterojunctions, *RSC Adv.*, 2017, **7**(28), 17387–17397.
8 Q. He, S. Wu, Z. Yin and H. Zhang, Graphene-based electronic sensors, *Chem. Sci.*, 2012, **3**(6), 1764–1772.
9 Y. Liu, X. Dong and P. Chen, Biological and chemical sensors based on graphene materials, *Chem. Soc. Rev.*, 2012, **41**(6), 2283–2307.
10 M. Chhowalla, D. Jena and H. Zhang, Two-dimensional semiconductors for transistors, *Nat. Rev. Mater.*, 2016, **1**(11), 1–15.
11 C. Gong, *et al.*, Electronic and optoelectronic applications based on 2D novel anisotropic transition metal dichalcogenides, *Adv. Sci.*, 2017, **4**(12), 1700231.
12 N. Joshi, T. Hayasaka, Y. Liu, H. Liu, J. Osvaldo, N. Oliviera and L. Lin, A review on chemiresistive room temperature gas sensors based on metal oxide nanostructures, graphene and 2D transition metal dichalcogenides, *Microchim. Acta*, 2018, **185**(4), 213.
13 E. Lee, Y. S. Yoon and D.-J. Kim, Two-dimensional transition metal dichalcogenides and metal oxide hybrids for gas sensing, *ACS Sens.*, 2018, **3**(10), 2045–2060.
14 W. Zheng, R. Lin, Z. Zhang and F. Hunag, Vacuum-ultraviolet photodetection in few-layered h-BN, *ACS Appl. Mater. Interfaces*, 2018, **10**(32), 27116–27123.
15 X. Wu, *et al.*, Thinnest nonvolatile memory based on monolayer h-BN, *Adv. Mater.*, 2019, **31**(15), 1806790.
16 F. Iacopi, J. J. Boeckl and C. Jagadish, *2D Materials*, Elsevier Ltd, 2016.
17 A. Özden, F. Ay, C. Sevik and N. K. Perkgöz, CVD growth of monolayer MoS_2: Role of growth zone configuration and precursors ratio, *Jpn. J. Appl. Phys.*, 2017, **56**, 6S1.
18 Y. Xie, *et al.*, Growth of monolayer WS_2 single crystals with atmospheric pressure CVD: Role of temperature, *MRS Adv.*, 2019, **4**(3–4), 255–262.
19 P. Sahatiya, S. S. Jones and S. Badhulika, Direct, large area growth of few-layered MoS_2 nanostructures on various flexible substrates: Growth kinetics and its effect on photodetection studies, *Flexible Print. Electron.*, 2018, **3**(1), 015002.
20 T. H. Choudhury, X. Zhang, Z. Y. A. Balushi, M. Chubarov and J. M. Redwing, Epitaxial growth of two-dimensional layered transition metal dichalcogenides, *Annu. Rev. Mater. Res.*, 2020, **50**, 155–177.
21 S. V. Mandyam, H. M. Kim and M. Drndic, Large area few-layer TMD film growths and their applications, *J. Phys.: Mater.*, 2020, **3**(2), 024008.
22 B. Kalanyan, *et al.*, Rapid wafer-scale growth of polycrystalline 2H-MoS_2 by pulsed metalorganic chemical vapor deposition, *Chem. Mater.*, 2017, **29**(15), 6279–6288.
23 N. Briggs, *et al.*, A roadmap for electronic grade 2D materials, *2D Mater.*, 2019, **6**(2), 022001.
24 M. Amani, *et al.*, Growth-substrate induced performance degradation in chemically synthesized monolayer MoS_2 field effect transistors, *Appl. Phys. Lett.*, 2014, **104**(20), 203506.
25 H. Li, Y. Li, A. Aljarb, Y. Shi and L.-J. Li, Epitaxial growth of two-dimensional layered transition-metal dichalcogenides: Growth mechanism, controllability, and scalability, *Chem. Rev.*, 2017, **18**(13), 6134–6150.
26 D. Neumaier, S. Pindi and M. C. Lemme, Integrating graphene into semiconductor fabrication lines, *Nat. Mater.*, 2019, **18**(6), 525–529.
27 A. Kozhakhmetov, *et al.*, Scalable BEOL compatible 2D tungsten diselenide, *2D Mater.*, 2019, **7**(1), 015209.
28 D. Akinwande, *et al.*, Graphene and two-dimensional materials for silicon technology, *Nature*, 2019, **573**(7775), 507–518.
29 L. A. Walsh and C. L. Hinkle, van der Waals epitaxy: 2D materials and topological insulators, *Appl. Mater. Today*, 2017, **9**, 504–515.
30 R. Addou and R. M. Wallace, Integration of 2D materials for advanced devices: Challenges and opportunities, *ECS Trans.*, 2017, **79**(1), 11–20.

31 S. Salahuddin, K. Ni and S. Datta, The era of hyper-scaling in electronics, *Nat. Electron.*, 2018, **1**(8), 442–450.
32 R. A. Potyrailo, Multivariable sensors for ubiquitous monitoring of gases in the era of internet of things and industrial internet, *Chem. Rev.*, 2016, **116**(19), 11877–11923.
33 Y. Zhan, Y. Mei and L. Zheng, Materials capability and device performance in flexible electronics for the Internet of Things, *J. Mater. Chem. C*, 2014, **2**(7), 1220–1232.
34 M. Swan, Sensor mania! The internet of things, wearable computing, objective metrics, and the quantified self 2.0, *J. Sens. Actuat. Netw.*, 2012, **1**(3), 217–253.
35 L. Roselli, *et al.*, Smart surfaces: Large area electronics systems for internet of things enabled by energy harvesting, *Proc. IEEE*, 2014, **102**(11,), 1723–1746.
36 A. O. Watanabe *et al.*, First demonstration of 28 GHz and 39 GHz transmission lines and antennas on glass substrates for 5G modules, presented at the IEEE 67th Electronic Components and Technology Conference, 2017.
37 A. O. Watanabe, T.-H. Lin, P. M. Raj, V. Sundaram, M. M. Tentzeris and R. R. Tummala, Leading-Edge and Ultra-Thin 3D Glass-Polymer 5G Modules with Seamless Antenna-to-Transceiver Signal Transmissions, presented at the IEEE 68th Electronic Components and Technology Conference, 2018.
38 A. B. Shorey and R. Lu, Progress and application of through glass via (TGV) technology, presented at the Pan Pacific Microelectronics Symposium, 2019.
39 D. Akinwande, N. Petrone and J. Hone, Two-dimensional flexible nanoelectronics, *Nat. Commun.*, 2014, **5**(1), 1–12.
40 G. A. Salvatore, *et al.*, Fabrication and transfer of flexible few-layers MoS_2 thin film transistors to any arbitrary substrate, *ACS Nano*, 2013, **7**(10), 8809–8815.
41 J. R. Nasr, N. Simonson, A. Oberoi, M. W. Horn, J. A. Robinson and S. Das, Low-power and ultra-thin MoS_2 photodetectors on glass, *ACS Nano*, 2020, **14**(11), 15440–15449.
42 L. L. Chang and K. Ploog, *Molecular Beam Epitaxy and Heterostructures*, SpringerLink, 1985.
43 H. Ohno, Ferromagnetic III–V heterostructures, *J. Vac. Sci. Technol., B: Microelectron. Nanometer Struct.–Process., Meas., Phenom.*, 2000, **18**(4), 2039–2043.
44 K. Y. Cheng, Development of molecular beam epitaxy technology for III–V compound semiconductor heterostructure devices, *J. Vac. Sci. Technol., A*, 2013, **31**(5), 50814.
45 L. A. Kolodziejski, R. L. Gunshor, A. V. Nurmikko and N. Otsuka, Molecular beam epitaxy of II-VI based heterostructures, *Acta Phys. Pol. A*, 1991, **79**(1), 31–47.
46 T. Roy, *et al.*, Field-effect transistors built from all two-dimensional material components, *ACS Nano*, 2014, **8**(6), 6259–6264.
47 M. Onodera, S. Masubuchi, R. Moriya and T. Machida, Assembly of van der Waals heterostructures: Exfoliation, searching, and stacking of 2D materials, *Jpn. J. Appl. Phys.*, 2020, **59**(1), 10101.
48 M. Wang, *et al.*, Manufacturing strategies for wafer-scale two-dimensional transition metal dichalcogenide heterolayers, *J. Mater. Res.*, 2020, **35**(11), 1350–1368.
49 K. Kim, *et al.*, van der Waals heterostructures with high accuracy rotational alignment, *Nano Lett.*, 2016, **16**(3), 1989–1995.
50 Y. Cao, *et al.*, Unconventional superconductivity in magic-angle graphene superlattices, *Nature*, 2018, **556**(7699), 43–50.
51 M. Yankowitz, *et al.*, Tuning superconductivity in twisted bilayer graphene, *Science*, 2019, **363**(6431), 1059–1064.
52 Y. Liu, Y. Huang and X. Duan, van der Waals integration before and beyond two-dimensional materials, *Nature*, 2019, **567**(7748), 323–333.
53 L.-P. Ma, W. Ren and H.-M. Cheng, Transfer Methods Of Graphene From Metal Substrates: A review, *Small Methods*, 2019, **3**(7), 1900049.
54 R. Frisenda, *et al.*, Recent progress in the assembly of nanodevices and van der Waals heterostructures by deterministic placement of 2D materials, *Chem. Soc. Rev.*, 2018, **47**(1), 53–68.
55 S. Fan, Q. A. Vu, M. D. Tran, S. Adhikari and Y. H. Lee, Transfer assembly for two-dimensional van der Waals heterostructures, *2D Mater.*, 2020, **7**(2), 022005.
56 A. J. Watson, W. Lu, M. H. D. Guimaraes and M. Stöhr, Transfer of large-scale two-dimensional semiconductors: Challenges and developments, *2D Mater.*, 2021, **8**(3), 032001.
57 P. Braeuninger-Weimer, *et al.*, Fast, noncontact, wafer-scale, atomic layer resolved imaging of two-dimensional materials by ellipsometric contrast micrography, *ACS Nano*, 2018, **12**(8), 8555–8563.
58 F. Zhang, C. Erb, L. Runkle, X. Zhang and N. Alem, Etchant-free transfer of 2D nanostructures, *Nanotechnology*, 2017, **29**(2), 025602.
59 D. Ma, *et al.*, A universal etching-free transfer of MoS_2 films for applications in photodetectors, *Nano Res.*, 2015, **8**(11), 3662–3672.
60 M. Sharma, A. Singh and R. Singh, Monolayer MoS_2 transferred on arbitrary substrates for potential use in flexible electronics, *ACS Appl. Nano Mater.*, 2020, **3**(5), 4445–4453.
61 Z. Lin, *et al.*, Controllable growth of large-size crystalline MoS_2 and resist-free transfer assisted with a Cu thin film, *Sci. Rep.*, 2016, **5**(1), 18596.
62 T. Ma, K. Miyazaki, H. Ariga, S. Takakusagi and K. Asakura, Investigation of the cleanliness of transferred graphene: The first step toward its application as a window material for electron microscopy and spectroscopy, *Bull. Chem. Soc. Jpn.*, 2015, **88**(8), 1029–1035.
63 Z. Tu, *et al.*, Controllable growth of 1–7 layers of graphene by chemical vapour deposition, *Carbon*, 2014, **73**, 252–258.
64 T. Zhang, *et al.*, Clean transfer of 2D transition metal dichalcogenides using cellulose acetate for atomic resolution characterizations, *ACS Appl. Nano Mater.*, 2019, **2**(8), 5320–5328.
65 J. Shim, *et al.*, Controlled crack propagation for atomic precision handling of wafer-scale two-dimensional materials, *Science*, 2018, **362**(6415), 665–670.

66 M. Graf, *et al.*, Fabrication and practical applications of molybdenum disulfide nanopores, *Nat. Protoc.*, 2019, **14**(4), 1130–1168.
67 H.-P. Komsa, J. Kotakoski, S. Kurasch, O. Lehtinen, U. Kaiser and A. V. Krasheninnikov, Two-dimensional transition metal dichalcogenides under electron irradiation: Defect production and doping, *Phys. Rev. Lett.*, 2012, **109**(3), 035503.
68 K. Liu, J. Feng, A. Kis and A. Radenovic, Atomically thin molybdenum disulfide nanopores with high sensitivity for DNA translocation, *ACS Nano*, 2014, **8**(3), 2504–2511.
69 Q. Xu, *et al.*, Controllable atomic scale patterning of free-standing monolayer graphene at elevated temperature, *ACS Nano*, 2013, **7**(2), 1566–1572.
70 H.-Y. Cho, T. K. Nguyen, F. Ullah, J.-W. Yun, C. K. Nguyen and Y. S. Kim, Salt-assisted clean transfer of continuous monolayer MoS_2 film for hydrogen evolution reaction, *Phys. B: Condensed Matter*, 2018, **532**, 84–89.
71 A. Gurarslan, *et al.*, Surface-energy-assisted perfect transfer of centimeter-scale monolayer and few-layer MoS_2 films onto arbitrary substrates, *ACS Nano*, 2014, **8**(11), 11522–11528.
72 A. Castellanos-Gomez, *et al.*, Deterministic transfer of two-dimensional materials by all-dry viscoelastic stamping, *2D Mater.*, 2014, **1**, 1.
73 K. F. Mak, C. Lee, J. Hone, J. Shan and T. F. Heinz, Atomically thin MoS_2: A new direct-gap semiconductor, *Phys. Rev. Lett.*, 2010, **105**(13), 136805.
74 X.-L. Li, W.-P. Han, J.-B. Wu, X.-F. Qiao, J. Zhang and P.-H. Tan, Layer-number dependent optical properties of 2D materials and their application for thickness determination, *Adv. Funct. Mater.*, 2017, **27**(19), 1604468.
75 L. Mennel, M. M. Furchi, S. Wachter, M. Paur, D. K. Polyushkin and T. Mueller, Optical imaging of strain in two-dimensional crystals, *Nat. Commun.*, 2018, **9**(1), 1–6.
76 J. D. Buron, *et al.*, Terahertz wafer-scale mobility mapping of graphene on insulating substrates without a gate, *Opt. Express*, 2015, **23**(24), 30721–30729.
77 A. Quellmalz, *et al.*, Large-area integration of two-dimensional materials and their heterostructures by wafer bonding, *Nat. Commun.*, 2021, **12**(1), 1–11.
78 L. Jiao, B. Fan, X. Xian, Z. Wu, J. Zhang and Z. Liu, Creation of nanostructures with poly(methyl methacrylate)-mediated nanotransfer printing, *J. Am. Chem. Soc.*, 2008, **130**(38), 12612–12613.
79 A. Reina, *et al.*, Transferring and identification of single- and few-layer graphene on arbitrary substrates, *J. Phys. Chem. C*, 2008, **112**(46), 17741–17744.
80 A. Reina, *et al.*, Large area, few-layer graphene films on arbitrary substrates by chemical vapor deposition, *Nano Lett.*, 2009, **9**(1), 30–35.
81 Z.-Q. Xu, *et al.*, Synthesis and transfer of large-area monolayer WS_2 crystals: Moving toward the recyclable use of sapphire substrates, *ACS Nano*, 2015, **9**(6), 6178–6187.
82 L. Zhang, *et al.*, Damage-free and rapid transfer of CVD-grown two-dimensional transition metal dichalcogenides by dissolving sacrificial water-soluble layers, *Nanoscale*, 2017, **9**(48), 19124–19130.
83 Z. Lin, *et al.*, Controllable growth of large-size crystalline MoS_2 and resist-free transfer assisted with a Cu thin film, *Sci. Rep.*, 2015, **5**(1), 1–10.
84 J. Kang, D. Shin, S. Bae and B. H. Hong, Graphene transfer: Key for applications, *Nanoscale*, 2012, **4**(18), 5527–5537.
85 X. Li, *et al.*, Transfer of large-area graphene films for high-performance transparent conductive electrodes, *Nano Lett.*, 2009, **9**(12), 4359–4363.
86 H. C. Lee, *et al.*, Review of the synthesis, transfer, characterization and growth mechanisms of single and multilayer graphene, *RSC Adv.*, 2017, **7**(26), 15644–15693.
87 A. L. Elías, *et al.*, Controlled synthesis and transfer of large-area WS_2 sheets: From single layer to few layers, *ACS Nano*, 2013, **7**(6), 5235–5242.
88 J. Shi, *et al.*, Controllable growth and transfer of monolayer MoS_2 on Au foils and its potential application in hydrogen evolution reaction, *ACS Nano*, 2014, **8**(10), 10196–10204.
89 X. Wang, *et al.*, Chemical vapor deposition growth of crystalline monolayer $MoSe_2$, *ACS Nano*, 2014, **8**(5), 5125–5131.
90 Q. Fu, *et al.*, Synthesis and enhanced electrochemical catalytic performance of monolayer $WS_{2(1-x)}Se_{2x}$ with a tunable band gap, *Adv. Mater.*, 2015, **27**(32), 4732–4738.
91 Y. Gong, *et al.*, Vertical and in-plane heterostructures from WS_2/MoS_2 monolayers, *Nat. Mater.*, 2014, **13**(12), 1135–1142.
92 J.-G. Song, *et al.*, Controllable synthesis of molybdenum tungsten disulfide alloy for vertically composition-controlled multilayer, *Nat. Commun.*, 2015, **6**(1), 1–10.
93 B. Li, *et al.*, Scalable transfer of suspended two-dimensional single crystals, *Nano Lett.*, 2015, **15**(8), 5089–5097.
94 Y. Lee, *et al.*, Wafer-scale synthesis and transfer of graphene films, *Nano Lett.*, 2010, **10**(2), 490–493.
95 Y.-C. Lin, *et al.*, Wafer-scale MoS_2 thin layers prepared by MoO_3 sulfurization, *Nanoscale*, 2012, **4**(20), 6637–6641.
96 D. G. Gilles and R. C. Loehr, Waste generation and minimization in semiconductor industry, *J. Environ. Eng.*, 1994, **120**(1), 72–86.
97 L. G. P. Martins, Y. Song, T. Zeng, M. S. Dresselhaus, J. Kong and P. T. Araujo, Direct transfer of graphene onto flexible substrates, *Proc. Natl. Acad. Sci. U. S. A.*, 2013, **110**(44), 17762–17767.
98 Z. Lu, *et al.*, Universal transfer and stacking of chemical vapor deposition grown two-dimensional atomic layers with water-soluble polymer mediator, *ACS Nano*, 2016, **10**(5), 5237–5242.
99 J. H. Kim, *et al.*, Centimeter-scale green integration of layer-by-layer 2D TMD vdW heterostructures on arbitrary substrates by water-assisted layer transfer, *Sci. Rep.*, 2019, **9**(1), 1–10.
100 G. F. Schneider, V. E. Calado, H. Zandbergen, L. M. K. Vandersypen and C. Dekker, Wedging transfer of nanostructures, *Nano Lett.*, 2010, **10**(5), 1912–1916.

101 V. E. Calado, G. F. Schneider, A. M. M. G. Theulings, C. Dekker and L. M. K. Vandersypen, Formation and control of wrinkles in graphene by the wedging transfer method, *Appl. Phys. Lett.*, 2012, **101**(10), 103116.
102 H. Li, J. Wu, X. Huang, Z. Yin, J. Liu and H. Zhang, A universal, rapid method for clean transfer of nanostructures onto various substrates, *ACS Nano*, 2014, **8**(7), 6563–6570.
103 M. Hong, *et al.*, Decoupling the interaction between wet-transferred MoS_2 and graphite substrate by an interfacial water layer, *Adv. Mater. Interfaces*, 2018, **5**, 21.
104 P. Wang, *et al.*, High-fidelity transfer of chemical vapor deposition grown 2D transition metal dichalcogenides *via* substrate decoupling and polymer/small molecule composite, *ACS Nano*, 2020, **14**(6), 7370–7379.
105 Y. Wang, *et al.*, Electrochemical delamination of CVD-grown graphene film: Toward the recyclable use of copper catalyst, *ACS Nano*, 2011, **5**(12), 9927–9933.
106 L. Gao, *et al.*, Repeated growth and bubbling transfer of graphene with millimetre-size single-crystal grains using platinum, *Nat. Commun.*, 2012, **3**(1), 1–7.
107 S. Koh, Y. Saito, H. Kodama and A. Sawabe, Epitaxial growth and electrochemical transfer of graphene on Ir(111)/α-Al_2O_3(0001) substrates, *Appl. Phys. Lett.*, 2016, **109**(2), 023105.
108 H. Cun, *et al.*, Centimeter-sized single-orientation monolayer hexagonal boron nitride with or without nanovoids, *Nano Lett.*, 2018, **18**(2), 1205–1212.
109 Y. Gao, *et al.*, Large-area synthesis of high-quality and uniform monolayer WS_2 on reusable Au foils, *Nat. Commun.*, 2015, **6**(1), 1–10.
110 Z. Zhang, *et al.*, Direct chemical vapor deposition growth and band-gap characterization of MoS_2/h-BN van der Waals heterostructures on Au foils, *ACS Nano*, 2017, **11**(4), 4328–4336.
111 A. Pirkle, *et al.*, The effect of chemical residues on the physical and electrical properties of chemical vapor deposited graphene transferred to SiO_2, *Appl. Phys. Lett.*, 2011, **99**(12), 122108.
112 J. W. Suk, *et al.*, Enhancement of the electrical properties of graphene grown by chemical vapor deposition via controlling the effects of polymer residue, *Nano Lett*, 2013, **13**(4), 1462–1467.
113 G. B. Barin, Y. Song, I. D. F. Gimenez, A. G. S. Filho, L. S. Barreto and J. Kong, Optimized graphene transfer: Influence of polymethylmethacrylate (PMMA) layer concentration and baking time on graphene final performance, *Carbon*, 2015, **84**, 82–90.
114 H. J. Jeong, *et al.*, Improved transfer of chemical-vapor-deposited graphene through modification of intermolecular interactions and solubility of poly(methylmethacrylate) layers, *Carbon*, 2014, **66**, 612–618.
115 A. Suhail, K. Islam, B. Li, D. Jenkins and G. Pan, Reduction of polymer residue on wet-transferred CVD graphene surface by deep UV exposure, *Appl. Phys. Lett.*, 2017, **110**(18), 183103.
116 R. Yang, X. Zheng, Z. Wang, C. J. Miller and P. X.-L. Feng, Multilayer MoS_2 transistors enabled by a facile dry-transfer technique and thermal annealing, *J. Vac. Sci. Technol., B: Microelectron. Nanometer Struct.–Process., Meas., Phenom.*, 2014, **32**(6), 061203.
117 K. Kumar, Y.-S. Kim and E.-H. Yang, The influence of thermal annealing to remove polymeric residue on the electronic doping and morphological characteristics of graphene, *Carbon*, 2013, **65**, 35–45.
118 D. Marinov, *et al.*, Reactive plasma cleaning and restoration of transition metal dichalcogenide monolayers, *NPJ 2D Mater. Appl.*, 2021, **5**(1), 1–10.
119 X. Liang, *et al.*, Toward clean and crackless transfer of graphene, *ACS Nano*, 2011, **5**(11), 9144–9153.
120 A. M. Goossens, V. E. Calado, A. Barreiro, K. Watanabe, T. Taniguchi and L. M. K. Vandersypen, Mechanical cleaning of graphene, *Appl. Phys. Lett.*, 2012, **100**(7), 073110.
121 N. Lindvall, A. Kalabukhov and A. Yurgens, Cleaning graphene using atomic force microscope, *J. Appl. Phys.*, 2012, **111**(6), 064904.
122 B. Zhuang, S. Li, S. Li and J. Yin, Ways to eliminate PMMA residues on graphene – superclean graphene, *Carbon*, 2021, **173**, 609–636.
123 W. H. Lee, *et al.*, Simultaneous transfer and doping of CVD-grown graphene by fluoropolymer for transparent conductive films on plastic, *ACS Nano*, 2012, **6**(2), 1284–1290.
124 W. S. Leong, *et al.*, Paraffin-enabled graphene transfer, *Nat. Commun.*, 2019, **10**(1), 1–8.
125 D. Zhang, *et al.*, A double support layer for facile clean transfer of two-dimensional materials for high-performance electronic and optoelectronic devices, *ACS Nano*, 2019, **13**(5), 5513–5522.
126 H. H. Kim, *et al.*, Clean transfer of wafer-scale graphene *via* liquid phase removal of polycyclic aromatic hydrocarbons, *ACS Nano*, 2015, **9**(5), 4726–4733.
127 A. Jain, *et al.*, Minimizing residues and strain in 2D materials transferred from PDMS, *Nanotechnology*, 2018, **29**, 26.
128 H. Jia, *et al.*, Single-and few-layer transfer-printed CVD MoS_2 nanomechanical resonators with enhancement by thermal annealing, in *2016 IEEE International Frequency Control Symposium (IFCS)*, 2016, IEEE, pp. 1–3, DOI: 10.1109/FCS.2016.7546737.
129 H. Yu, *et al.*, Wafer-scale growth and transfer of highly-oriented monolayer MoS_2 continuous films, *ACS Nano*, 2017, **11**(12), 12001–12007.
130 A. Singh, M. Moun, M. Sharma, A. Barman, A. K. Kapoor and R. Singh, NaCl-Assisted substrate dependent 2D planar nucleated growth of MoS_2, *Appl. Surf. Sci.*, 2021, **538**, 148201.
131 S. S. Han, *et al.*, Automated assembly of wafer-scale 2D TMD heterostructures of arbitrary layer orientation and stacking sequence using water dissoluble salt substrates, *Nano Lett*, 2020, **20**(5), 3925–3934.
132 Y.-H. Lee, *et al.*, Synthesis and transfer of single-layer transition metal disulfides on diverse surfaces, *Nano Lett*, 2013, **13**(4), 1852–1857.
133 J. Kim, *et al.*, Layer-resolved graphene transfer *via* engineered strain layers, *Science*, 2013, **342**(6160), 833–836.

134 S. B. Desai, *et al.*, Gold-mediated exfoliation of ultralarge optoelectronically-perfect monolayers, *Adv. Mater.*, 2016, **28**(21), 4053–4058.
135 S.-H. Bae, *et al.*, Unveiling the carrier transport mechanism in epitaxial graphene for forming wafer-scale, single-domain graphene, *Proc. Natl. Acad. Sci. U. S. A.*, 2017, **114**(16), 4082–4086.
136 L. Song, L. Ci, W. Gao and P. M. Ajayan, Transfer printing of graphene using gold film, *ACS Nano*, 2009, **3**(6), 1353–1356.
137 S. Lai, J. Jeon, Y.-J. Song and S. Lee, Water-penetration-assisted mechanical transfer of large-scale molybdenum disulfide onto arbitrary substrates, *RSC Adv*, 2016, **6**(62), 57497–57501.
138 Z. Xu and M. J. Buehler, Interface structure and mechanics between graphene and metal substrates: A first-principles study, *J. Phys.: Condens. Matter*, 2010, **22**, 48.
139 T. Björkman, A. Gulans, A. V. Krasheninnikov and R. M. Nieminen, van der Waals bonding in layered compounds from advanced density-functional first-principles calculations, *Phys. Rev. Lett.*, 2012, **108**(23), 235502.
140 S. K. Hong, S. M. Song, O. Sul and B. J. Cho, Carboxylic group as the origin of electrical performance degradation during the transfer process of CVD growth graphene, *J. Electrochem. Soc.*, 2012, **159**(4), K107–K109.
141 P. Ahlberg, *et al.*, Defect formation in graphene during low-energy ion bombardment, *APL Mater.*, 2016, **4**(4), 046104.
142 C.-T. Chen, E. A. Casu, M. Gajek and S. Raoux, Low-damage high-throughput grazing-angle sputter deposition on graphene, *Appl. Phys. Lett.*, 2013, **103**(3), 033109.
143 F. O. L. Johansson, P. Ahlberg, U. Jansson, S.-L. Zhang, A. Lindblad and T. Nyberg, Minimizing sputter-induced damage during deposition of WS_2 onto graphene, *Appl. Phys. Lett.*, 2017, **110**(9), 091601.
144 M. Higo, K. Fujita, Y. Tanaka, M. Mitsushio and T. Yoshidome, Surface morphology of metal films deposited on micaat various temperatures observed by atomic force microscopy, *Appl. Surf. Sci.*, 2006, **252**(14), 5083–5099.
145 J. A. Thornton, The microstructure of sputter-deposited coatings, *J. Vac. Sci. Technol., A*, 1986, **4**(6), 3059–3065.
146 L. Wang, *et al.*, One-dimensional electrical contact to a two-dimensional material, *Science*, 2013, **342**(6158), 614–617.
147 K. Kinoshita, *et al.*, Dry release transfer of graphene and few-layer h-BN by utilizing thermoplasticity of polypropylene carbonate, *NPJ 2D Mater. Appl.*, 2019, **3**(1), 1–8.
148 K. Kang, *et al.*, Layer-by-layer assembly of two-dimensional materials into wafer-scale heterostructures, *Nature*, 2017, **550**(7675), 229–233.
149 Z. Ying, *et al.*, Superlubricity enabled dry transfer of non-encapsulated graphene, *Chin. Phys. B*, 2019, **28**(2), 028102.
150 T. Iwasaki, *et al.*, Bubble-free transfer technique for high-quality graphene/hexagonal boron nitride van der Waals heterostructures, *ACS Appl. Mater. Interfaces*, 2020, **12**(7), 8533–8538.
151 S. Son, *et al.*, Strongly adhesive dry transfer technique for van der Waals heterostructure, *2D Mater.*, 2020, **7**(4), 41005.
152 D. G. Purdie, N. M. Pugno, T. Taniguchi, K. Watanabe, A. C. Ferrari and A. Lombardo, Cleaning interfaces in layered materials heterostructures, *Nat. Commun.*, 2018, **9**(1), 1–12.
153 S. Masubuchi, *et al.*, Autonomous robotic searching and assembly of two-dimensional crystals to build van der Waals superlattices, *Nat. Commun.*, 2018, **9**(1), 1–12.
154 S.-J. Yang, S. Choi, F. O. O. Ngome, K.-J. Kim, S.-Y. Choi and C.-J. Kim, All-dry transfer of graphene film by van der Waals interactions, *Nano Lett.*, 2019, **19**(6), 3590–3596.
155 G. Lupina, *et al.*, Residual metallic contamination of transferred chemical vapor deposited graphene, *ACS Nano*, 2015, **9**(5), 4776–4785.
156 A. V. Zaretski, *et al.*, Metal-assisted exfoliation (MAE): Green, roll-to-roll compatible method for transferring graphene to flexible substrates, *Nanotechnology*, 2015, **26**(4), 045301.
157 S.-H. Bae, *et al.*, Integration of bulk materials with two-dimensional materials for physical coupling and applications, *Nat. Mater.*, 2019, **18**(6), 550–560.
158 I. Constant, F. Tardif and J. Derrien, Deposition and removal of sodium contamination on silicon wafers, *Semicond. Sci. Technol.*, 1999, **15**(1), 61–66.
159 L. Banszerus, *et al.*, Ultrahigh-mobility graphene devices from chemical vapor deposition on reusable copper, *Sci. Adv.*, 2015, **1**(6), e1500222.
160 S. Bae, *et al.*, Roll-to-roll production of 30 inch graphene films for transparent electrodes, *Nat. Nanotechnol.*, 2010, **5**(8), 574–578.
161 J. Kang, *et al.*, Efficient transfer of large-area graphene films onto rigid substrates by hot pressing, *ACS Nano*, 2012, **6**(6), 5360–5365.
162 G. H. Han, H.-J. Shin, E. S. Kim, S. J. Chae, J.-Y. Choi and Y. H. Lee, Poly(ethylene-*co*-vinyl acetate)-assisted one-step transfer of ultra-large graphene, *Nano*, 2011, **6**(1), 59–65.
163 K. Kanahashi, J. Pu and T. Takenobu, 2D materials for large-area flexible thermoelectric devices, *Adv. Energy Mater*, 2019, **10**(11), 1902842.
164 D. Akinwande, N. Petrone and J. Hone, Two-dimensional flexible nanoelectronics, *Nat. Commun.*, 2014, **5**, 5678.
165 T. Sekitani, *et al.*, Organic nonvolatile memory transistors for flexible sensor arrays, *Science*, 2009, **326**(5959), 1516–1519.
166 W. N. Zhu, S. Park, M. N. Yogeesh and D. Akinwande, Advancements in 2D flexible nanoelectronics: from material perspectives to RF applications, *Flexible Print. Electron.*, 2017, **2**(4), 043001.
167 S. Das, R. Gulotty, A. V. Sumant and A. Roelofs, All two-dimensional, flexible, transparent, and thinnest thin film transistor, *Nano Lett.*, 2014, **14**(5), 2861–2866.
168 S. J. Kim, K. Choi, B. Lee, Y. Kim and B. H. Hong, Materials for flexible, stretchable electronics: Graphene and 2D materials, *Annu. Rev. Mater. Res.*, 2015, **45**(1), 63–84.
169 A. Dodda, S. Subbulakshmi Radhakrishnan, T. F. Schranghamer, D. Buzzell, P. Sengupta and S. Das, Graphene-based physically unclonable functions that are

reconfigurable and resilient to machine learning attacks, *Nat. Electron.*, 2021, **4**(5), 364–374.
170 A. Wali, S. Kundu, A. J. Arnold, G. Zhao, K. Basu and S. Das, Satisfiability attack-resistant camouflaged two-dimensional heterostructure devices, *ACS Nano*, 2021, **15**(2), 3453–3467.
171 A. Sebastian, A. Pannone, S. Subbulakshmi Radhakrishnan and S. Das, Gaussian synapses for probabilistic neural networks, *Nat. Commun.*, 2019, **10**(1), 1–11.
172 S. Subbulakshmi Radhakrishnan, A. Sebastian, A. Oberoi, S. Das and S. Das, A biomimetic neural encoder for spiking neural network, *Nat. Commun.*, 2021, **12**(1), 2143.
173 D. Jayachandran, *et al.*, A low-power biomimetic collision detector based on an in-memory molybdenum disulfide photodetector, *Nat. Electron.*, 2020, **3**(10), 646–655.
174 T. F. Schranghamer, A. Oberoi and S. Das, Graphene memristive synapses for high precision neuromorphic computing, *Nat. Commun.*, 2020, **11**(1), 5474.
175 A. Dodda, A. Oberoi, A. Sebastian, T. H. Choudhury, J. M. Redwing and S. Das, Stochastic resonance in MoS_2 photodetector, *Nat. Commun.*, 2020, **11**(1), 4406.
176 S. Das, A. Dodda and S. Das, A biomimetic 2D transistor for audiomorphic computing, *Nat. Commun.*, 2019, **10**(1), 3450.
177 A. J. Arnold, T. Shi, I. Jovanovic and S. Das, Extraordinary radiation hardness of atomically thin MoS_2, *ACS Applied Materials & Interfaces*, 2019, **11**(8), 8391–8399.
178 C. Choi, *et al.*, Curved neuromorphic image sensor array using a MoS_2–organic heterostructure inspired by the human visual recognition system, *Nat. Commun.*, 2020, **11**(1), 5934.
179 X. Zhu, D. Li, X. Liang and W. D. Lu, Ionic modulation and ionic coupling effects in MoS_2 devices for neuromorphic computing, *Nat. Mater.*, 2019, **18**(2), 141–148.
180 J. Jiang, *et al.*, 2D MoS_2 neuromorphic devices for brain-like computational systems, *Small*, 2017, **13**, 29.
181 E. Singh, P. Singh, K. S. Kim, G. Y. Yeom and H. S. Nalwa, Flexible molybdenum disulfide (MoS_2) atomic layers for wearable electronics and optoelectronics, *ACS Appl. Mater. Interfaces*, 2019, **11**(12), 11061–11105.
182 S. Gupta, W. T. Navaraj, L. Lorenzelli and R. Dahiya, Ultra-thin chips for high-performance flexible electronics, *NPJ Flexible Electron.*, 2018, **2**(1), 1–17.
183 E. Okogbue, *et al.*, Centimeter-scale periodically corrugated few-layer 2D MoS_2 with tensile stretch-driven tunable multifunctionalities, *ACS Appl. Mater. Interfaces*, 2018, **10**(36), 30623–30630.
184 Z. Pan, N. Liu, L. Fu and Z. Liu, Wrinkle engineering: A new approach to massive graphene nanoribbon arrays, *J. Am. Chem. Soc.*, 2011, **133**(44), 17578–17581.
185 C. J. An, *et al.*, Ultraclean transfer of CVD-grown graphene and its application to flexible organic photovoltaic cells, *J. Mater. Chem. A*, 2014, **2**(48), 20474–20480.
186 N. Joshi, T. Hayasaka, Y. Liu, H. Liu, J. Osvaldo, N. Oliviera and L. Lin, A review on chemiresistive room temperature gas sensors based on metal oxide nanostructures, graphene and 2D transition metal dichalcogenides, *Microchim. Acta*, 2018, **185**(4), 1–16.
187 Y. Wang, S. W. Tong, X. F. Xu, B. Özyilmaz and K. P. Loh, Interface engineering of layer-by-layer stacked graphene anodes for high-performance organic solar cells, *Adv. Mater.*, 2011, **23**(13), 1514–1518.
188 L.-P. Ma, *et al.*, UV-epoxy-enabled simultaneous intact transfer and highly efficient doping for roll-to-roll production of high-performance graphene films, *ACS Appl. Mater. Interfaces*, 2018, **10**(47), 40756–40763.
189 G. Spierings, Wet chemical etching of silicate glasses in hydrofluoric acid based solutions, *J. Mater. Sci.*, 1993, **28**(23), 6261–6273.
190 H. K. Jang, Y. D. Chung, S. W. Whangbo, I. W. Lyo and C. N. Whang, Effects of chemical etching with hydrochloric acid on a glass surface, *J. Vac. Sci. Technol., A*, 2000, **18**(5), 2563–2567.
191 G.-H. Lee, *et al.*, Flexible and transparent MoS_2 field-effect transistors on hexagonal boron nitride-graphene heterostructures, *ACS Nano*, 2013, **7**(9), 7931–7936.
192 L. Britnell, *et al.*, Field-effect tunneling transistor based on vertical graphene heterostructures, *Science*, 2012, **335**(6071), 947–950.
193 S. Bertolazzi, D. Krasnozhon and A. Kis, Nonvolatile memory cells based on MoS_2/graphene heterostructures, *ACS Nano*, 2013, **7**(4), 3246–3252.
194 T. Georgiou, *et al.*, Vertical field-effect transistor based on graphene–WS_2 heterostructures for flexible and transparent electronics, *Nat. Nanotechnol*, 2013, **8**(2), 100–103.
195 I. V. Sankar, J. Jeon, S. K. Jang, J. H. Cho, E. Hwang and S. Lee, Heterogeneous integration of 2D materials: Recent advances in fabrication and functional device applications, *Nano*, 2019, **14**(12), 1930009.
196 T. Uwanno, Y. Hattori, T. Taniguchi, K. Watanabe and K. Nagashio, Fully dry PMMA transfer of graphene on h-BN using a heating/cooling system, *2D Mater.*, 2015, **2**, 4.
197 D. Rhodes, S. H. Chae, R. Ribeiro-Palau and J. Hone, Disorder in van der Waals heterostructures of 2D materials, *Nat. Mater.*, 2019, **18**(6), 541–549.
198 K. T. He, J. D. Wood, G. P. Doidge, E. Pop and J. W. Lyding, Scanning tunneling microscopy study and nanomanipulation of graphene-coated water on mica, *Nano Lett*, 2012, **12**(6), 2665–2672.
199 J. Shim, *et al.*, Water-gated charge doping of graphene induced by mica substrates, *Nano Lett.*, 2012, **12**(2), 648–654.
200 K. Xu, P. Cao and J. R. Heath, Graphene visualizes the first water adlayers on mica at ambient conditions, *Science*, 2010, **329**(5996), 1188–1191.
201 Z. Peng, R. Yang, M. A. Kim, L. Li and H. Liu, Influence of O_2, H_2O and airborne hydrocarbons on the properties of selected 2D materials, *RSC Adv*, 2017, **7**(43), 27048–27057.
202 A. Ambrosi and M. Pumera, The CVD graphene transfer procedure introduces metallic impurities which alter the graphene electrochemical properties, *Nanoscale*, 2014, **6**(1), 472–476.
203 S. J. Haigh, *et al.*, Cross-sectional imaging of individual layers and buried interfaces of graphene-based

heterostructures and superlattices, *Nat. Mater.*, 2012, **11**(9), 764–767.

204 A. V. Kretinin, *et al.*, Electronic properties of graphene encapsulated with different two-dimensional atomic crystals, *Nano Lett*, 2014, **14**(6), 3270–3276.

205 F. Pizzocchero, *et al.*, The hot pick-up technique for batch assembly of van der Waals heterostructures, *Nat. Commun.*, 2016, **7**(1), 1–10.

206 M. R. Rosenberger, H.-J. Chuang, K. M. McCreary, A. T. Hanbicki, S. V. Sivaram and B. T. Jonker, Nano-squeegee for the creation of clean 2D material interfaces, *ACS Appl. Mater. Interfaces*, 2018, **10**(12), 10379–10387.

207 S. Chen, *et al.*, Tip-based cleaning and smoothing improves performance in monolayer MoS_2 devices, *ACS Omega*, 2021, **6**, 4013–4021.

208 Z. Liu, A. A. Bol and W. Haensch, Large-scale graphene transistors with enhanced performance and reliability based on interface engineering by phenylsilane self-assembled monolayers, *Nano Lett*, 2010, **11**(2), 523–528.

209 A. Castellanos-Gomez, *et al.*, Isolation and characterization of few-layer black phosphorus, *2D Mater*, 2014, **1**(2), 025001.

210 Y. Cao, *et al.*, Quality heterostructures from two-dimensional crystals unstable in air by their assembly in inert atmosphere, *Nano Lett.*, 2015, **15**(8), 4914–4921.

211 S. Pace, *et al.*, Synthesis of large-scale monolayer 1T′-$MoTe_2$ and its stabilization *via* scalable hBN encapsulation, *ACS Nano*, 2021, **15**(3), 4213–4225.

212 G. Mirabelli, *et al.*, Air sensitivity of MoS_2, $MoSe_2$, $MoTe_2$, HfS_2, and $HfSe_2$, *J. Appl. Phys.*, 2016, **120**(12), 125102.

213 Q. Li, Q. Zhou, L. Shi, Q. Chen and J. Wang, Recent advances in oxidation and degradation mechanisms of ultrathin 2D materials under ambient conditions and their passivation strategies, *J. Mater. Chem. A*, 2019, **7**(9), 4291–4312.

214 X. Zhang, F. Jia, B. Yang and S. Song, Oxidation of molybdenum disulfide sheet in water under *in situ* atomic force microscopy observation, *J. Phys. Chem. C*, 2017, **121**(18), 9938–9943.

215 T. Choi, S. J. Kim, S. Park, T. Hwang, Y. Jeon and B. H. Hong, Roll-to-roll synthesis and patterning of graphene and 2D materials, presented at the IEEE International Electron Devices Meeting, 2015.

216 C. Cai, *et al.*, Crackless transfer of large-area graphene films for superiorperformance transparent electrodes, *Carbon*, 2016, **98**, 457–462.

217 M. Hempel, *et al.*, Repeated roll-to-roll transfer of two-dimensional materials by electrochemical delamination, *Nanoscale*, 2018, **10**(12), 5522–5531.

218 B. N. Chandrashekar, *et al.*, Roll-to-roll green transfer of CVD graphene onto plastic for a transparent and flexible triboelectric nanogenerator, *Adv. Mater.*, 2015, **27**(35), 5210–5216.

219 P. R. Whelan, *et al.*, Raman spectral indicators of catalyst decoupling for transfer of CVD grown 2D materials, *Carbon*, 2017, **117**, 75–81.

220 D. Luo, *et al.*, Role of graphene in water-assisted oxidation of copper in relation to dry transfer of graphene, *Chem. Mater.*, 2017, **29**(10), 4546–4556.

221 R. Wu, L. Gan, X. Ou, Q. Zhang and Z. Luo, Detaching graphene from copper substrate by oxidation-assisted water intercalation, *Carbon*, 2016, **98**, 138–143.

222 A. Shivayogimath, *et al.*, Do-it-yourself transfer of large-area graphene using an office laminator and water, *Chem. Mater.*, 2019, **31**(7), 2328–2336.

223 P. Yang, *et al.*, Batch production of 6 inch uniform monolayer molybdenum disulfide catalyzed by sodium in glass, *Nat. Commun.*, 2018, **9**(1), 1–10.

224 L. Oakes, T. Hanken, R. Carter, W. Yates and C. L. Pint, Roll-to-roll nanomanufacturing of hybrid nanostructures for energy storage device design, *ACS Appl. Mater. Interfaces*, 2015, **7**(26), 14201–14210.

225 R. A. Wells, H. Johnson, C. R. Lhermitte, S. Kinge and K. Sivula, Roll-to-roll deposition of semiconducting 2D nanoflake films of transition metal dichalcogenides for optoelectronic applications, *ACS Appl. Nano Mater*, 2019, **2**(12), 7705–7712.

226 Y. R. Lim, *et al.*, Roll-to-roll production of layer-controlled molybdenum disulfide: A platform for 2D semiconductor-based industrial applications, *Adv. Mater.*, 2018, **30**(5), 1705270.

